5. THE OXIDATION MECHANISM OF TITANIA SLAG

5.1 Introduction

The previous chapters detail the development of the BTS process. The most important part of the BTS process is the oxidation roast because significant phase and chemical changes occur during this process stage that determine the success of the entire process. During oxidation the M_3O_5 phase in the as-cast slag is transformed to rutile/anatase (TiO_2), iron-rich M_3O_5 and M_2O_3. In the process the Ti(III) and Fe(II) that are present in the as-cast slag are oxidised to Ti(IV) and Fe(III). Iron migration to the outside rims of the slag particles is another important morphological change that occurs during the oxidation of titania slag. This renders the iron easily accessible to the leach solution in subsequent processing. This chapter focuses on the mechanism of titania slag oxidation in an attempt to explain the observed chemical and morphological changes.

5.2 Background

5.2.1 Segregation and diffusion of elements in oxide systems

The segregation of impurities in oxides to grain boundaries and surfaces is a common occurrence. Kingery (1984) found that Ca segregates in MgO as a result of the misfit strains generated by the Ca ion substituting for MgO. Cook (1988) found that Ca also segregates in Al_2O_3 for the same reason. When aliovalent impurities (impurities having more than one oxidation state) are present in ionic solids the driving force for segregation can be the electrostatic potential present at grain boundaries and surfaces. Due to the formation of cation and anion vacancies the boundaries of an ionic solid will carry an electric charge caused by the presence of excess ions of one sign. A compensating charge of the opposite sign adjacent to the boundary would then be created. An example of segregation by this mechanism can be found in the Sc(III)-MgO system (Chiang, 1981). Pint (1998) investigated the diffusion of rare earth impurities (RE) in Al_2O_3. He found that the RE impurities segregated to the grain boundaries from where it diffused to the oxide gas interface. There it accumulated until the solubility limit was exceeded. Following that the R.E. impurities were precipitated as separate particles. Pint found that the segregation of the R.E. impurities to the grain boundaries occurred as a result of a misfit of ions, but that the migration to the surface of the oxide occurred as a result of an oxygen potential gradient through the Al_2O_3.

5.2.2 Diffusion of Fe in TiO_2

The iron-titanium mixed oxide system has been the subject of several investigations as a result of its use as a photocatalyst (Bickley et al., 1991, Bickley et al., 1994 and Nobile and Davis, 1989). Amorelli et al. (1987) prepared polycrystalline TiO_2 powders treated with low levels (~200 ppm) of Fe(III). They showed that Fe(III) placed on the surface of rutile will migrate into the lattice when subjected to temperatures in excess of 400 °C. They also found that Fe(III) placed on the surface of anatase migrated into the lattice at high temperatures, but the migration did not take place to the same degree as found for rutile. This suggested that the structure of anatase is permeable to entry by Fe(III) but it was more difficult in comparison with rutile. The reason for the migration of the iron was

the concentration gradient of iron that existed between the insides and the outsides of the particles. Bickley et al. (1994) also prepared TiO_2 powders with 0.5 to 5 atom % Fe(III) ions on the surfaces of the particles. They found that the Fe(III) migrated into the particles at 500 °C. At temperatures in excess of 500 °C they found that Fe(III) that had previously migrated into the particles segregated back to the particle surfaces to form ferric pseudobrookite and hematite in addition to the solid solution of Fe(III) in TiO_2. They suggested that this surface enrichment occurred because the solubility limit of Fe(III) in TiO_2 had been exceeded. Bickley et al. (1991) reported that the solubility limit of Fe(III) in TiO_2 at 500 °C is in the region of 3 atom %. They found that Fe(III) is incorporated substitutionally in the TiO_2 matrix and that the solubility limit of Fe(III) is higher in rutile than it is in anatase.

5.3 Oxidation of titaniferous materials

5.3.1 Thermodynamics

As-cast titania slag contains mainly the $FeTi_2O_5$-Ti_3O_5 solid solution (ferrous M_3O_5) phase because the slag is quenched during casting. This phase is thermodynamically stable at the casting temperature of the slag (~1700 °C), but the phase composition of the slag is meta-stable at the roasting temperatures that were investigated during the process development for the production of BTS. This fact is illustrated by Figure 59, a part of the phase diagram for the system Ti-O-Fe at 1000 °C. The chemical composition of as-cast titania slag is indicated with a star on the diagram. At this temperature the thermodynamically stable phases for titania slag may be reduced rutile and metallic iron at a certain oxygen potential and not the ferrous M_3O_5 that is present in the slag. During oxidation the phase composition of the slag changes along the dotted line as oxygen is added to the material. This is a tie line between the chemical composition of the as-cast slag and oxygen. For oxidation in dilute air the phase composition of the slag will change along this line until it reaches the oxygen isobar in the rutile-pseudobrookite phase field that corresponds with the oxygen potential of the oxidising gas. The intersection between the tie line and the oxygen isobar representing an oxidising gas containing 5 % oxygen was calculated (Appendix XVI). This indicated that a partial oxygen pressure of 0.043 atm (corresponding to 5% oxygen at 0.86 atm) yields an equilibrium M_3O_5 solid solution with the mole fraction of ferric pseudobrookite in the Fe_2TiO_5-$FeTi_2O_5$ mixture equal to 0.997. The equilibrium products of slag oxidation in this gas hence are essentially pure ferric pseudobrookite and rutile.

From Figure 59 it can be predicted that the phase composition of as-cast titania slag may change during oxidation from ferrous M_3O_5 to:

1. a mixture of rutile, ilmenite and metallic iron;
2. a mixture of rutile and ilmenite-hematite solid solution;
3. a mixture of rutile, ilmenite-hematite solid solution and ferrous pseudobrookite solid solution and;
4. a mixture of rutile, and pseudobrookite solid solution.

The effect of temperature on the phase diagram is shown by Figure 60. It can be seen that the size of the rutile, ilmenite-hematite solid solution stability area increases dramatically as the temperature decreases. Another important effect is the formation, at lower temperatures, of an area where pseudobrookite solid solution, hematite solid solution and rutile are the stable phases. These changes in the phase stability areas can influence the phase changes that occur in titania slag during oxidation and reduction.

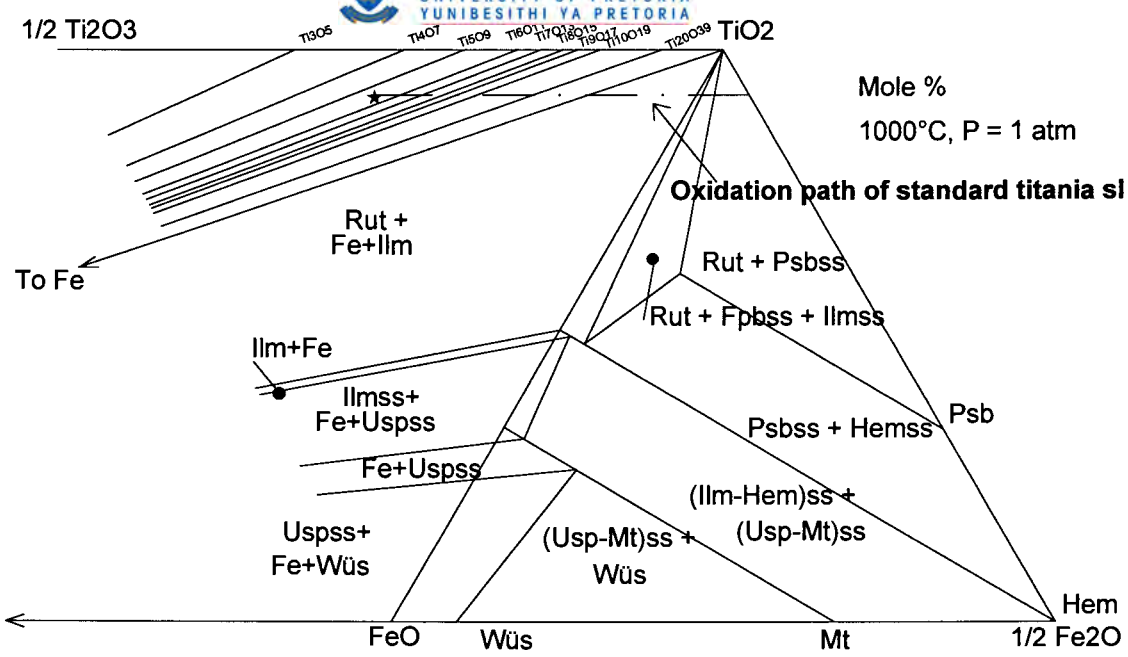

Figure 59. Part of the Ti-O-Fe phase diagram at 1000 °C (compiled from phase diagrams produced by Lindsley, 1976 and Ericksson and Pelton, 1996). A star indicates the chemical composition of as-cast slag and the oxidation path of this material is indicated by a dotted line.

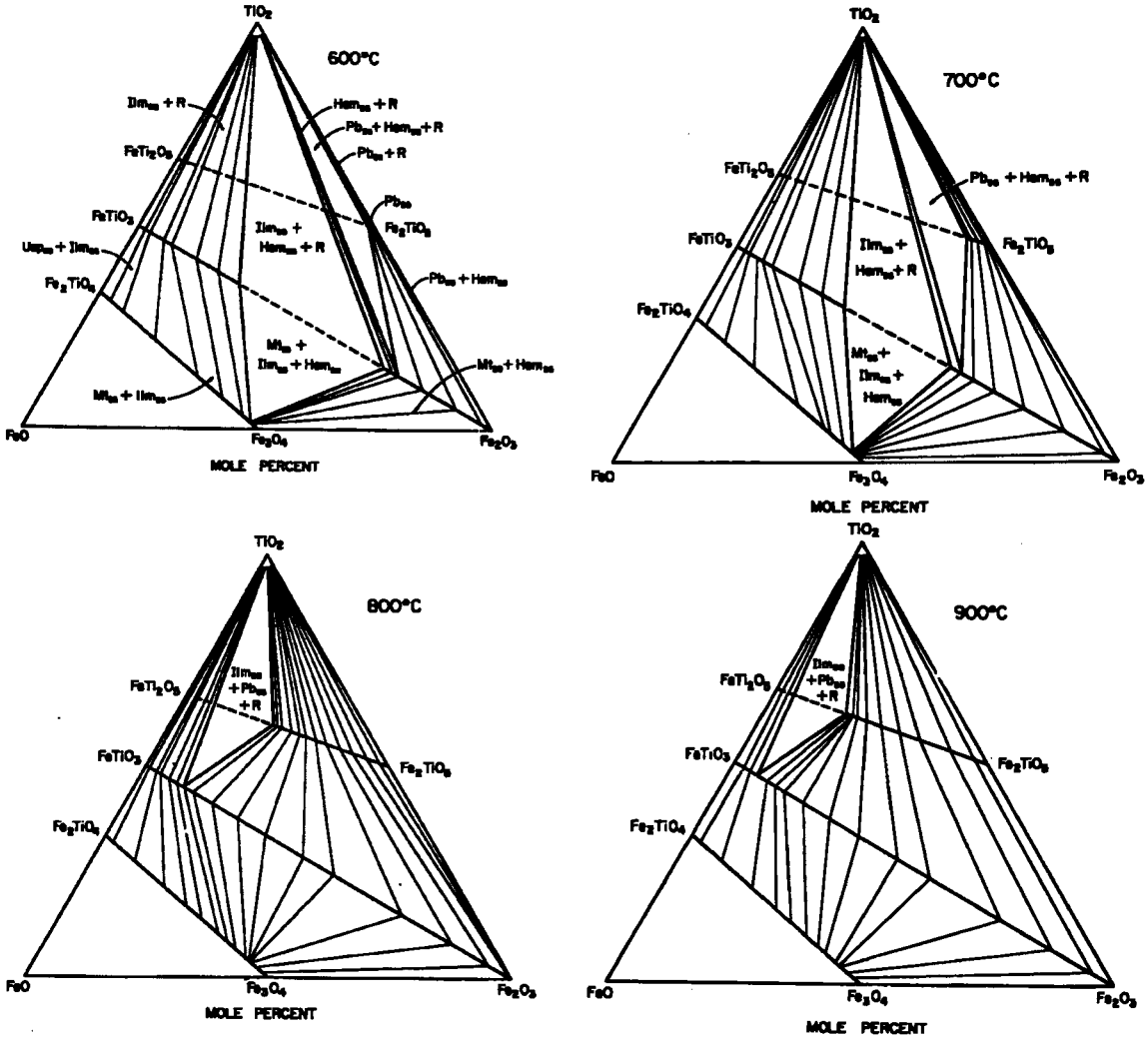

Figure 60. The effect of temperature on the TiO_2-FeO-Fe_2O_3 phase diagram (Haggerty, 1976).

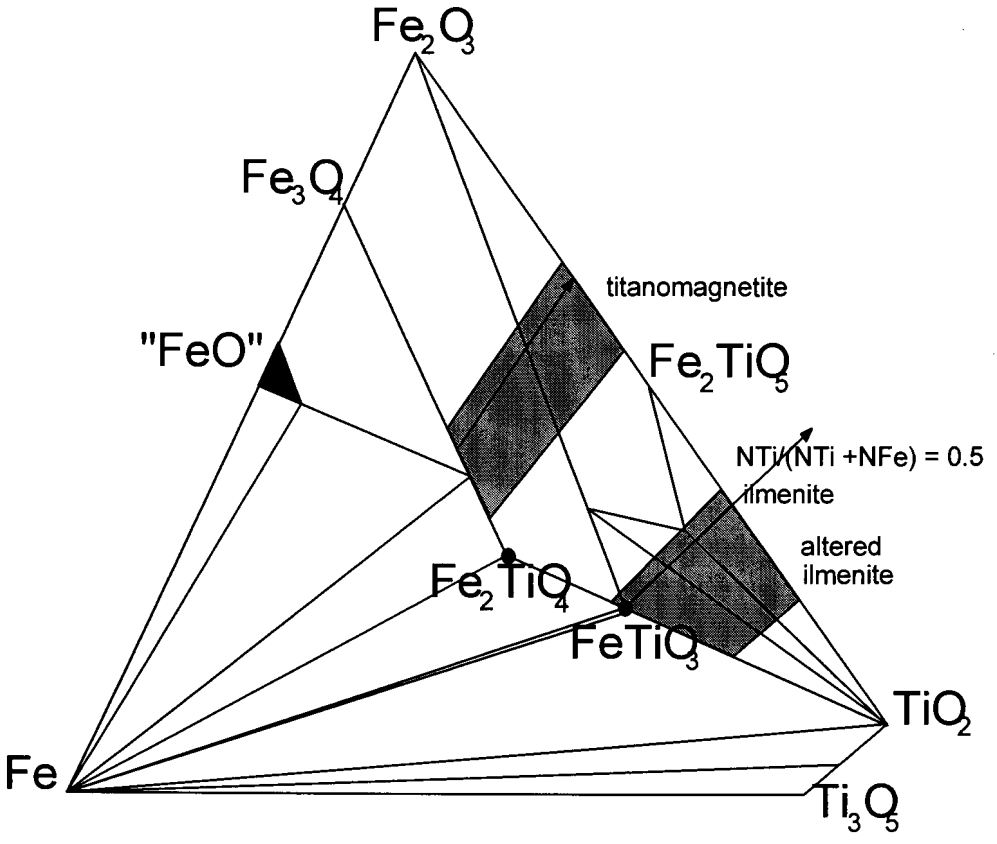

Figure 61. The isotherm of the Fe-Fe_2O_3-TiO_2 system at 800 °C (after Borowiec and Rosenqvist, 1981).

Literature data on ilmenite and titanomagnetite oxidation may shed some light on the possible phase transformations and hence are briefly reviewed here. The phase changes that occur during oxidation of ilmenite and titanomagnetite can be compared by examining Figure 61. This shows a part of the Fe-O-Ti phase diagram at 800 °C.

The theoretical composition of ilmenite, indicated by $FeTiO_3$, is shown in Figure 61. During oxidation oxygen is added to the material while the ratio of titanium to iron remains constant. Hence, the equilibrium phase composition of theoretically pure ilmenite subjected to oxidation $N_{Ti}/(N_{Ti} + N_{Fe}) = 0.5$ (with N the molar concentration). For other ilmenite ore compositions it moves along the band of lines with $N_{Ti}/(N_{Ti} + N_{Fe})$ varying between 0.48 - 0.68 depending on the degree of alteration of the ore (Lynd et al, 1954). During oxidation at 800 °C the composition changes upward to the right, along the lines. The equilibrium phase composition of material with a composition close to that of theoretical ilmenite changes from ilmenite to:

1. a mixture containing rutile/anatase (TiO_2) and ilmenite-hematite solid solution (M_2O_3);
2. a mixture containing rutile/anatase (TiO_2), pseudobrookite ($FeTi_2O_5$-$FeTi_2O_5$) solid solution and ilmenite-hematite solid solution (M_2O_3) and;
3. a mixture containing pseudobrookite solid solution ($FeTi_2O_5$-Fe_2TiO_5) and rutile/anatase (TiO_2).

Titanomagnetite is a solid solution between ulvöspinel and magnetite with the following formula: $xFe_2TiO_4.(1-x)Fe_3O_4$, x varies between 0.547 for unreacted material and 0.838 for oxidised material (Akimoto, 1984). This lies in the band of lines indicated by $N_{Ti}/(N_{Ti} + N_{Fe})$ = 0.18-0.28. During oxidation at 800°C the phase composition changes from titanomagnetite along a constant titanium to iron line to:

1. a mixture containing titanomagnetite (M_3O_4), and ilmenite-hematite solid solution (M_2O_3) and;
2. a mixture containing ilmenite-hematite solid solution (M_2O_3) and pseudobrookite solid solution (M_3O_5).

5.3.2 Kinetics of titania slag oxidation

Kinetic factors during oxidation result in phase and morphological changes that can not be predicted by phase equilibria. A detailed study on the oxidation of titania slag between 750 °C and 950 °C was conducted in Chapters 3 and 4. It was found that iron diffused to exposed surfaces of the slag particles during oxidation. This resulted in particles with TiO_2 rich cores surrounded by iron rich rims. XRD-analysis indicated that the original ferrous M_3O_5 is converted to rutile, anatase and Fe_2TiO_5-$FeTi_2O_5$ solid solution (M_3O_5) phase. Mössbauer spectroscopy indicated that the intermediate transformation phase ilmenite-hematite solid solution that is predicted by the phase diagram also form during oxidation, but contrary to the phase diagram the M_2O_3 phase in the form of hematite remains in the particles after extended reaction times as a meta-stable phase. The morphological investigation showed that the iron rich rims surrounding the particles consisted of two distinct phases that were probably ferric M_3O_5 and hematite. A phase change that was not expected was the formation of metallic iron and rutile around cracks in the unreacted particle cores. This appeared to form as a result of the oxidation of the Ti(III), that was in excess of the solubility limit for pseudobrookite at the roasting temperature, by Fe(II) and is predicted by the phase diagram in Figure 56 for a situation where no oxidation occurs.

5.3.3 Kinetics of ilmenite oxidation

Rao and Rigaud (1974) investigated the product morphology of oxidised ilmenite. Hematite was formed on the surface of the particles during oxidation below 770 °C. They proposed that Fe(II) migrated through the ilmenite to the hematite-ilmenite interface where it was oxidised. During oxidation between 770 °C and 900 °C hematite still formed on the surface, but a pseudorutile ($Fe_2Ti_3O_9$) layer was formed directly under the hematite. They proposed that the Fe(II) was oxidised to Fe(III) in the pseudorutile layer before it was precipitated as hematite on the outer surface. During oxidation above 900 °C ferric pseudobrookite was found close to the surface under a layer of rutile. They suggested that the mobility of titanium increase above 900 °C and that this result in TiO_2 on the surface. Briggs and Sacco (1993) investigated the oxidation of ilmenite with synthetic ilmenite discs at temperatures between 775 °C and 1000 °C. They did not find pseudorutile in any of their samples but they did find that rutile and ilmenite-hematite solid solution formed on the insides of the discs, while a pseudobrookite-rich layer formed closer to the surface of the discs. The outer surface of the discs always consisted of hematite. They suggested that the hematite layer formed by outward cation diffusion.

5.3.4 Kinetics of titanomagnetite oxidation

The oxidation of titanomagnetite has proved to be an integral part in studies about magnetic anomalies on the sea floor (Rayll and Hall, 1980). O'Reilly and Banerjee (1966) and Readman and O'Reilly (1972) found that oxidation was not a simple process without any changes in the relative cation content. Instead the process is accompanied

by iron diffusion out of the original oxide lattice. They suggested the following oxidation mechanism: Cations diffusing through the crystal lattice combine with adsorbed oxygen atoms at the surface which are ionised by the extra electrons from the Fe(II) ions. The speed at which the reaction occurs depends on the rate of diffusion of the cations. The cation distribution of oxidised single phase spinel is such that the tetrahedral sites are shared by Fe(II) and Fe(III). The octahedral sites are occupied by Ti (IV), Fe(II) and vacancies. Chemical bonding in the tetrahedral sites is not ionic but covalent as a result of the fact that covalent bonding at these sites lowers the lattice energy. This means that oxidation occurs largely at the expense of octahedral Fe(II). During the adsorption and ionisation of each oxygen atom on average 3/4 new tetrahedral sites and 1/2 new octahedral sites are formed that must be partially filled by cations. Those most likely to fill the new sites are the Fe(II) which have diffused to surface and transformed to Fe(III) cations during ionisation of the oxygen atom. When all octahedral Fe(II) ions have been oxidised the reaction can only proceed by the oxidation of tetrahedral Fe(II) and this results in the decomposition of the cation deficient spinel.

5.4 Proposed mechanism of titania slag oxidation

A summary of the phase and chemical changes that occur in titania slag during oxidation is shown in Figure 62. The three main zones represented are the unreacted core, the TiO_2-rich mantle zone and the iron-rich rim. The unreacted core consists of ferrous M_3O_5. The TiO_2-rich zone consists predominantly of anatase and rutile and the iron-rich zone consists predominantly of ferric pseudobrookite and hematite. In the process iron migrates to the outside rims of the slag particles, while Ti(III) and Fe(II) are oxidised to Ti(IV) and Fe(III).

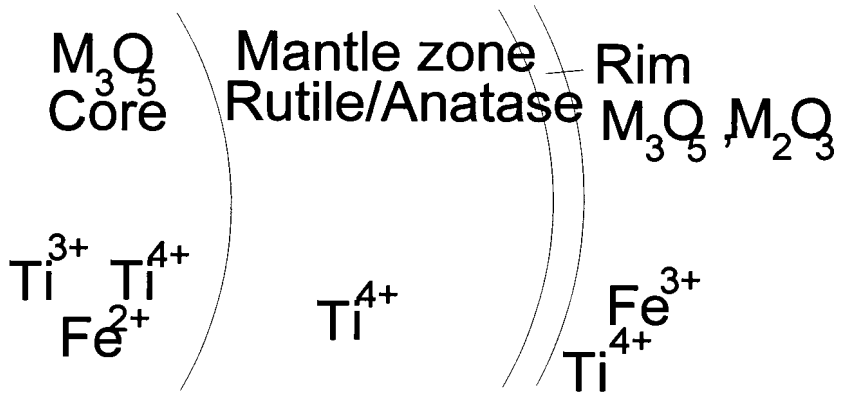

Figure 62. Summary of the phase and chemical changes that occurs in titania slag during oxidation.

Iron migration during oxidation of titania slag is a significant phenomenon. Three causes for the segregation or diffusion of elements in oxide systems have been identified in the background study:

1. The presence of bulk strains generated by the misfit of impurity ions in the crystal structure;
2. The existence of space charge effects as a result of the presence of aliovalent impurities in the oxide;
3. The presence of a chemical potential gradient between the insides and the outsides of the particles.

The first two causes listed above do not seem to be applicable in this system. For segregation to occur by the misfit of impurity ions the phase composition of the sample should stay the same. During oxidation of titania slag the original M_3O_5 phase is completely destroyed. Segregation of iron therefore cannot occur in the original M_3O_5 phase. Segregation by space charge effects is also not plausible as segregation by this mechanism only occurs over relatively short distances within the same phase. Migration of iron in titania slag takes place over several hundred microns through more than one phase. The most probable cause for the migration of iron to the outside surfaces of titania slag particles during oxidation is the presence of a chemical potential gradient between the insides and outsides of the particles.

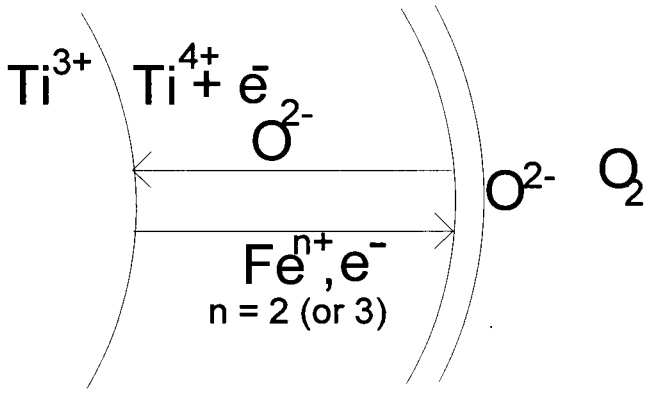

Figure 63. Proposed mechanism for the oxidation of titania slag.

Based on the summary of the chemical and morphological changes presented in Figure 62, the movement of cations and ions in the slag during oxidation can be inferred (Figure 63). Oxygen is reduced on the surface of the particles and diffuses into the interior, where the Ti(III) is oxidised and precipitated as rutile or anatase. The iron migrates to the surface of the particles as either Fe(II) or Fe(III) depending on where it is oxidised.

One possible reason for the observed morphology might be as a result of a large difference in the relative mobility of iron cations and oxygen anions, i.e. the iron cations precipitate at the outer surface because of their inherently higher diffusivity. This however seems unlikely, as the oxygen anions are able to diffuse through the product layer to precipitate rutile or anatase inside the particles, indicating substantial oxygen anion mobility. Another reason might be related to the formation of the M_2O_3 phase. The phase diagram predicts that this phase will form as an intermediate product during oxidation (See also Appendix XVII). The Mössbauer results shown in Chapter 4 confirmed that M_2O_3 formed. It was however still present in significant quantities in the slag at the end of the oxidation roast. The thermodynamic evaluation in paragraph 5.3.1 showed that this phase is more stable at lower roasting temperatures. The crystal structure of the M_2O_3 phase differs radically from the rutile and pseudobrookite phases that are present in the slag. Nucleation of the M_2O_3 phase would therefore require a large amount of nucleation energy. The nucleation energy that is required can be reduced if the M_2O_3 phase forms on a free surface. This can only occur on the outsides of the slag particles. Migration of iron cations to the surface of the particles therefore presumably determines where M_2O_3 precipitates.

5.5 Experimental plan

The experiments were planned around the following concepts:

- Roasting in the presence and in the absence of oxygen to determine whether oxygen is required for iron migration;
- Investigation into size and porosity changes during oxidation and reduction of titania slag;
- Coating slag particles with a marker material - to investigate the way oxygen is added to the particles;
- Evaluation of previously conducted line chemical analysis on roasted slag to determine the speciation of iron and titanium in the slag through phase fitting of the data;
- Leaching roasted slag under various conditions and measuring the speciation of iron in solution to determine the speciation of iron in the slag at different positions;
- Testing the influence of the iron rich rim on the mechanism of oxidation;
- Roasting at higher temperatures - to determine if there is a change in roasting mechanism and;
- Interrupted roasting - to test if this changes the mechanism.

5.6 Experimental procedure

5.6.1 Roasting

The roasting procedure was similar to that described in Chapter 4.

5.6.2 Leaching

The leach experimental procedure was similar to that described in Chapter 4 except for the reduction leach experiments where 31.5 g $SnCl_2.2H_2O$ were added to the leach solution per 50 g slag.

5.7 Results and Discussion

5.7.1 Investigation into the roasting conditions required for iron migration

Three experiments were designed to test whether a high oxygen potential is required for iron migration to occur in titania slag. For the first experiment slag was roasted in 100 % oxygen for 2 h at 850 °C. The second roast experiment was conducted in air and the third roast experiment was conducted in argon (containing < 2 ppm O_2). Micrographs of the slags after roasting are shown in Figure 64 and Table 47 gives the phase compositions.

Table 47. Phase composition of the slag samples roasted in 100 % O_2, air and argon at 850 °C for 2 h

Description	Mineralogical composition		
	Main	Minor	Trace
Slag roasted in 100% O_2	Anatase; Rutile	FeTi-Oxide	-
Slag roasted in air	Rutile, Anatase	FeTi-Oxide	-
Slag roasted in argon	FeTi-Oxide	Rutile	Iron

Legend: *FeTi-Oxide – M_3O_5 solid solution; Rutile – TiO_2; Anatase – TiO_2; Ilmenite – $FeTiO_3$; Iron – Fe*

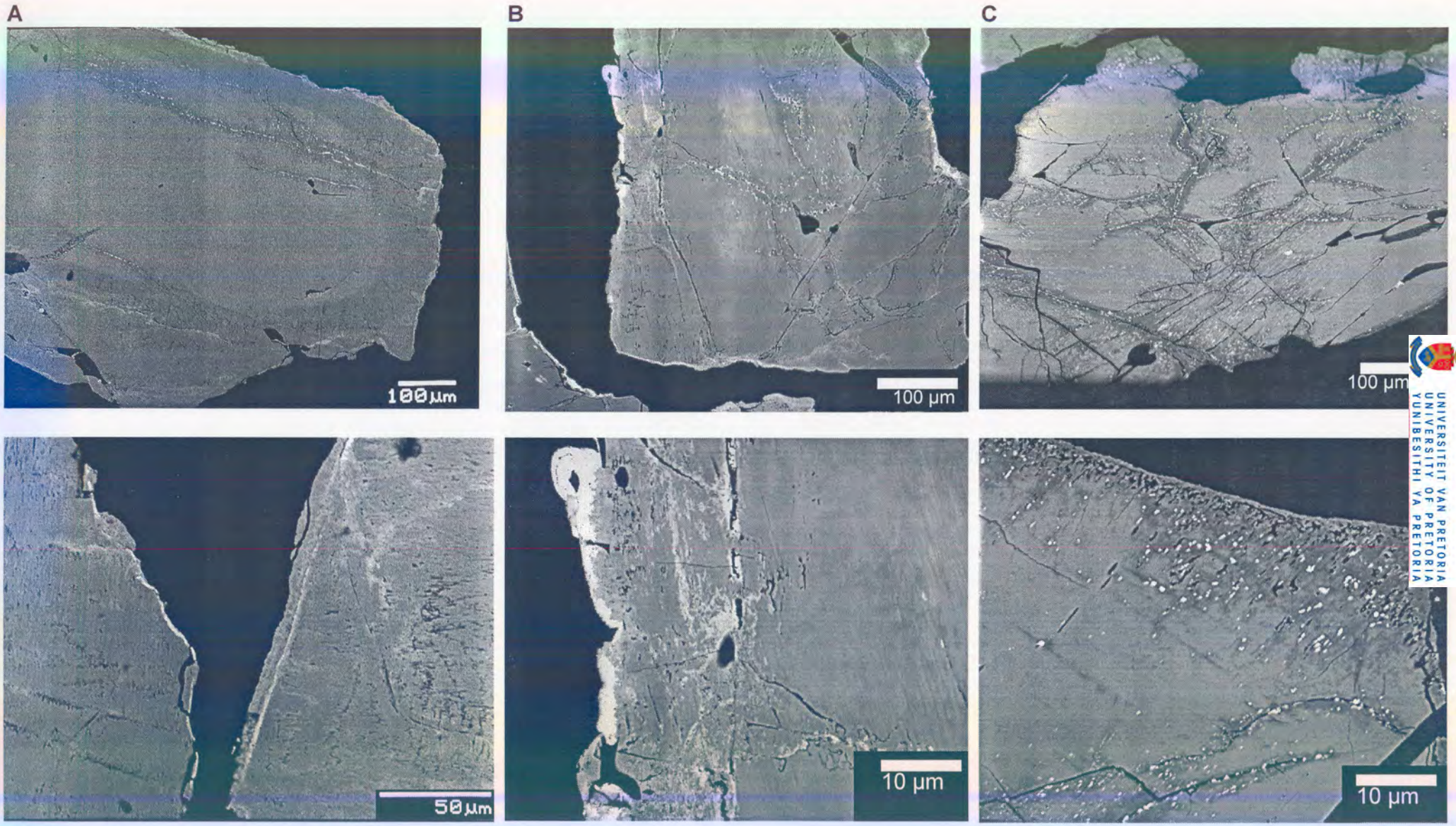

Figure 64. Slag roasted for 2 h at 850 °C. Oxygen was used to roast sample A, air was used for sample B and argon was used for sample C.

According to the results obtained by XRD-analysis, the slag roasted at 850 °C for 2 h in a 100 % O_2 atmosphere, consisted predominantly of anatase and rutile with lesser amounts of the M_3O_5 solid solution phase. The individual slag particles had a similar optical appearance to the titania slag particles roasted in air at 850 °C. The majority of slag particles displayed a well-defined zoned texture with unreacted M_3O_5-rich cores, TiO_2-rich mantle zones and thin iron enriched outer rims. Some of the slag particles were however completely transformed to TiO_2 with finely porous structure and iron enriched outer rims.

The slag particles roasted in air also had a similar well-defined zoned texture with iron enrichment towards the outer rims of the particles, a broad TiO_2-rich mantle zone and relatively small unreacted M_3O_5-rich cores.

The optical appearance of slag roasted in argon was completely different from the slag roasted in oxygen and air. The slag particles contained large unreacted cores consisting of the M_3O_5 solid solution phase displaying a relatively smooth and dense appearance. In addition, the slag particles contained relatively thin reaction zones along their outer margins as well as along cracks cutting through the unreacted M_3O_5-rich cores. These reaction zones consisted primarily of rutile as well as extremely fine-grained disseminated metallic iron precipitates. No iron migration occurred towards the outer rims of the slag particles.

These results can be explained by referring to the Ti-Fe-O phase diagram (Figure 59). The different phase compositional areas on the diagram are in equilibrium with gas mixtures of different oxygen potentials. In paragraph 5.3.1 it was shown that at equilibrium slag roasted in air will consist of the phases M_3O_5 and rutile. On the other hand the oxygen potential in argon is essentially an inert gas and this means that the oxidation kinetics is very slow. Based on these results roasting in oxygen rich atmospheres appear to be necessary for iron migration to occur.

5.7.2 Porosity and particle size changes during roasting

During oxidation oxygen is added to the slag and during reduction oxygen is removed. One would therefore expect the average particle size of the material to change during roasting. To investigate this the size distribution of the same slag sample was determined after crushing, oxidation and reduction. The results are presented in Figure 65. During oxidation the average particle size of the sample increased from a D_{50} of 463 µm to 471 µm. After reduction the average particle size decreased again to a D_{50} of 465 µm. An additional factor that influences the particle size is the introduction of pores in the material during roasting. Table 48 gives the porosity of the slag sample after crushing, oxidation and reduction. The as-cast slag is fairly dense with a porosity of only 0.0601 cm^3/g. During oxidation the porosity increases to 0.1397 cm^3/g and during reduction it increases further to 0.1433 cm^3/g. The particle size and porosity data supports the proposed oxidation mechanism. As oxygen is added to the material and iron migrates to the outsides of the particles the average particle size of the slag increases. This increases the porosity in the slag.

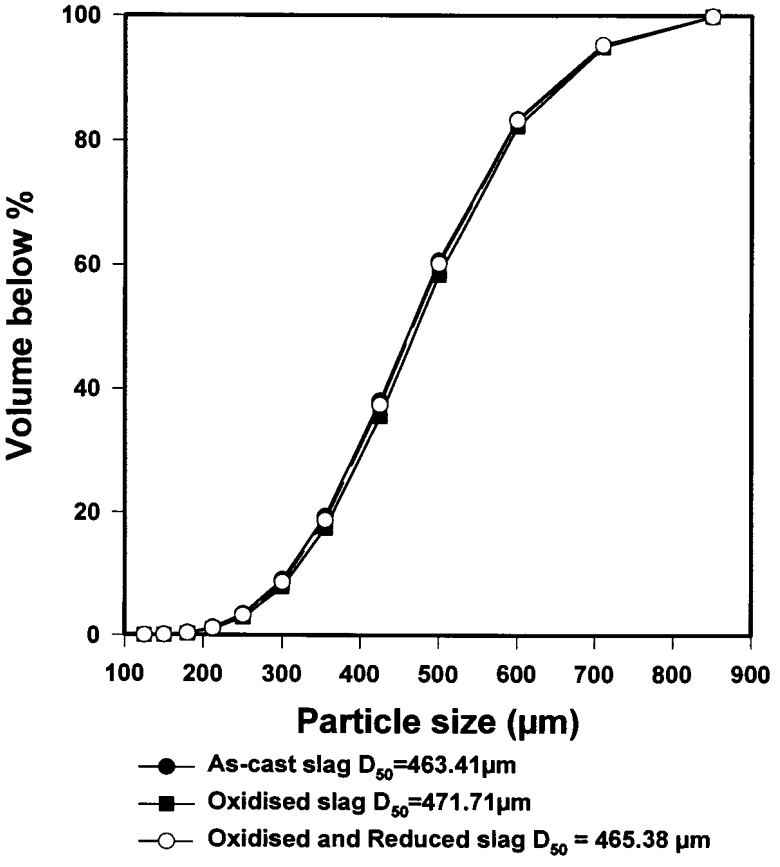

Figure 65. Particle size changes during roasting of titania slag.

Table 48. Porosity of slag particles before and after the roasting stages.

Description	Porosity (cm^3/g)
As-cast slag	0.0604
Oxidised slag	0.1397
Oxidised and reduced slag	0.1433

** Determined with a Micromeritics 9300 mercury porosimeter*

5.7.3 Investigation into the oxidation of coated slag particles

To investigate the migration of iron and titanium during oxidation an experiment was devised whereby the individual as-cast slag particles were coated with a marker material in order to observe the movement of cations. Gold was chosen as marker material and a few slag particles were sputter coated with gold (on average 0.5 to 1 µm thick). The gold-coated particles were mixed with uncoated particles that acted as a reference, and oxidised for 30 min at 850 °C in air. The phase chemical composition of the sample as determined by XRD-analysis is given in Table 49. Figure 66 shows micrographs of the sample after oxidation.

Table 49. Phase composition of the gold coated titania slag roasted in air at 850 °C for 30 min.

Description	Mineralogical composition		
	Main	Minor	Trace
Gold coated sample	Rutile; Anatase; FeTi-Oxide	-	Hematite

Legend : Rutile - TiO_2; Anatase - TiO_2; FeTi-Oxide -M_3O_5-solid solution; Hematite - Fe_2O_3

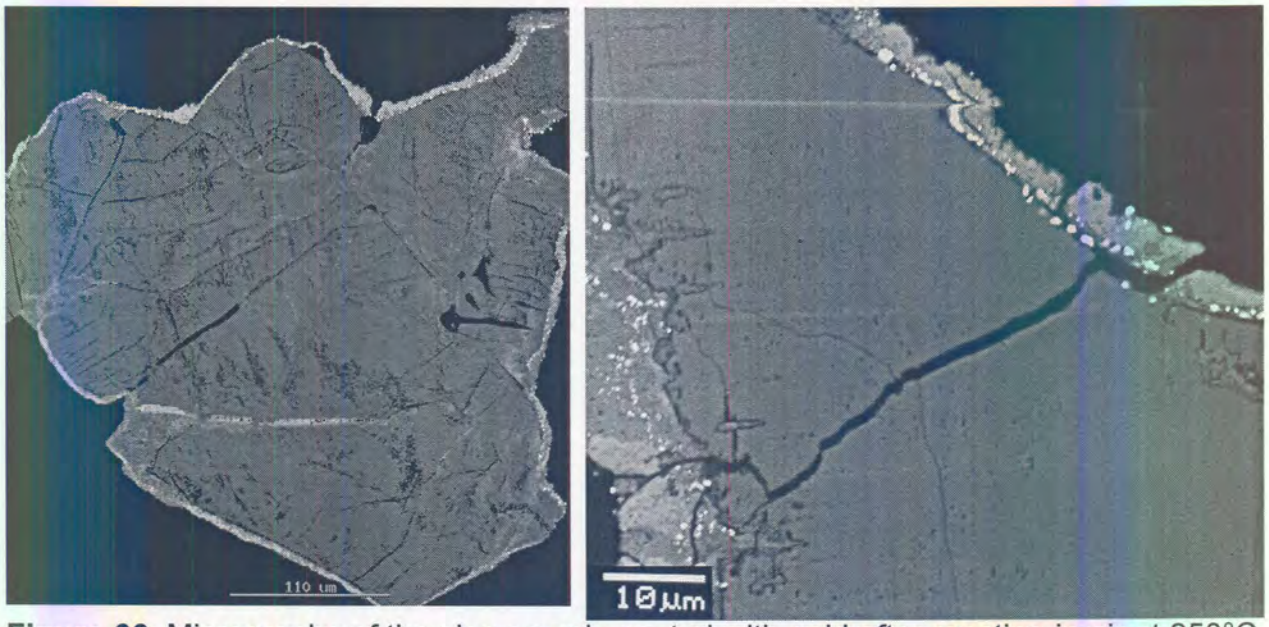

Figure 66. Micrographs of the slag sample coated with gold after roasting in air at 850°C for 30 min.

Optically the gold-coated slag particles had a well-defined zoned texture and appeared to be finely porous. The majority of slag particles were characterised by the occurrence of small, partially oxidised, M_3O_5-rich cores with relatively broad TiO_2-rich mantle zones and thin iron enriched outer rims. Some of the slag particles were however completely oxidised and transformed to TiO_2. These completely oxidised slag particles still displayed thin, but well-defined iron enriched outer rims. Remnants of the original gold layer, sputter coated onto the outer surfaces of the slag particles, was preserved and was observed during both optical microscopy as well as SEM investigation. This gold coated layer, originally situated at the outer rims of the individual titania slag particles, was now situated at the outer rim of the TiO_2-rich mantle zones, between the mantle and iron enriched outer layer of the slag particles. The outer rims of the slag particles appeared to be dual phased as two optically different phases could be distinguished. According to the results obtained during SEM investigation the higher reflecting phase (abundant phase) situated at the outer rims of the oxidised slag particles, represents a very high iron containing phase, probably hematite and/or titano-hematite, with the lower reflecting phase containing lesser amounts of iron-oxide with appreciable amounts of titania. This result supports the suggested oxidation mechanism of iron migration towards the surfaces of the particles and oxygen anions towards the interiors of the particles where Ti(III) is oxidised.

5.7.4 Investigation into the oxidation state of iron at various positions in oxidised slag particles

5.7.4.1 WDS point chemical analysis

Wavelength dispersive spectroscopy (WDS) analyses along lines through oxidised slag particles were conducted as part of the process development investigation in Chapter 4. These analyses showed that iron migrated to the outsides of the particles during oxidation. Based on the phases identified in the slag by XRD and the point chemical analyses it was possible to tentatively assign a phase composition to each of the points that were analysed. Basically one of three phases, glass, rutile or M_3O_5 was assigned to a point. Glass was assigned if the SiO_2 content exceeded 1 %. Rutile was assigned if the FeO content was below 4 % and all other analyses were assigned to M_3O_5. The chemical analyses of the points assigned to M_3O_5 were mathematically forced to fit stoichiometrically into the M_3O_5 formula. The amount of oxygen below or above the stoichiometric amount allowed the oxidation states of iron and titanium to be calculated. The results are presented in Figure 67. This shows that the unreacted cores contained about 10 % FeO. The iron is present in the Fe(II) oxidation state and the titanium in the Ti(IV) and Ti(III) oxidation states. In the TiO_2-rich mantle zone the FeO content varies between 0 % and 4 %. Iron is present in the Fe(II) oxidation state and titanium in the Ti(IV) and Ti(III) oxidation states. In the iron-rich rim the FeO content increases to about 50 %. The iron is present in rim in the Fe(II) oxidation state and the titanium in the Ti(IV) and Ti(III) states except for the extreme outer part where all iron is present in the Fe(III) oxidation state and all the titanium is in the Ti(IV) oxidation state.

This data showed that rutile precipitated from the original M_3O_5 phase during oxidation. In the process the remaining ferrous M_3O_5 phase gets enriched in iron and this can act as a driving force for the migration of iron to the outside surface of the particles or to local pores where ferric M_3O_5 can precipitate by the oxidation of Fe(II) (and the associated extra precipitation of rutile). This is tentatively confirmed by the observed iron concentration gradient through the mantle zone (Chapter 4).

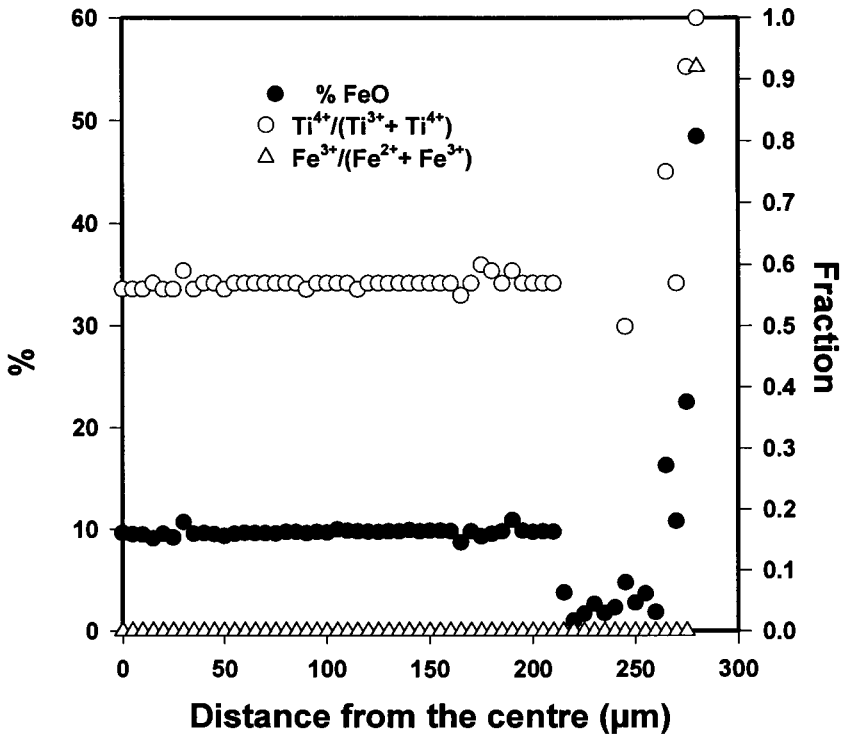

Figure 67. Variation of iron concentration, iron oxidation state and titanium oxidation state along a line through an oxidised slag particle.

5.7.4.2 Leach investigation

These experiments were designed as an alternative to the WDS investigation to determine the oxidation state of iron in the TiO_2-rich mantle zones that exist between the cores of unreacted M_3O_5 and the iron rich rims in oxidised titania slag particles. The areas in question had a relatively low iron concentration, but the iron migrates from the cores through this zone to the iron rich rims during oxidation.

Initially the following experiments were conducted: Titania slag was oxidised for 45 min at 850 °C in an atmosphere containing 10 % O_2. The slag was then subjected to leaching in boiling 20 % hydrochloric acid for various periods. To aid leaching $SnCl_2$ was added as a reductant. The aim of these experiments was to determine the leach time that was required to remove the iron rich-rims from the slag particles. Figure 68 shows the effect of leaching on the morphology of the samples. The iron-rich rims appeared to have been removed in all the samples. With extended leaching times the mantle zones became slightly more porous, but the unreacted cores were unaffected even after 8 h of leaching.

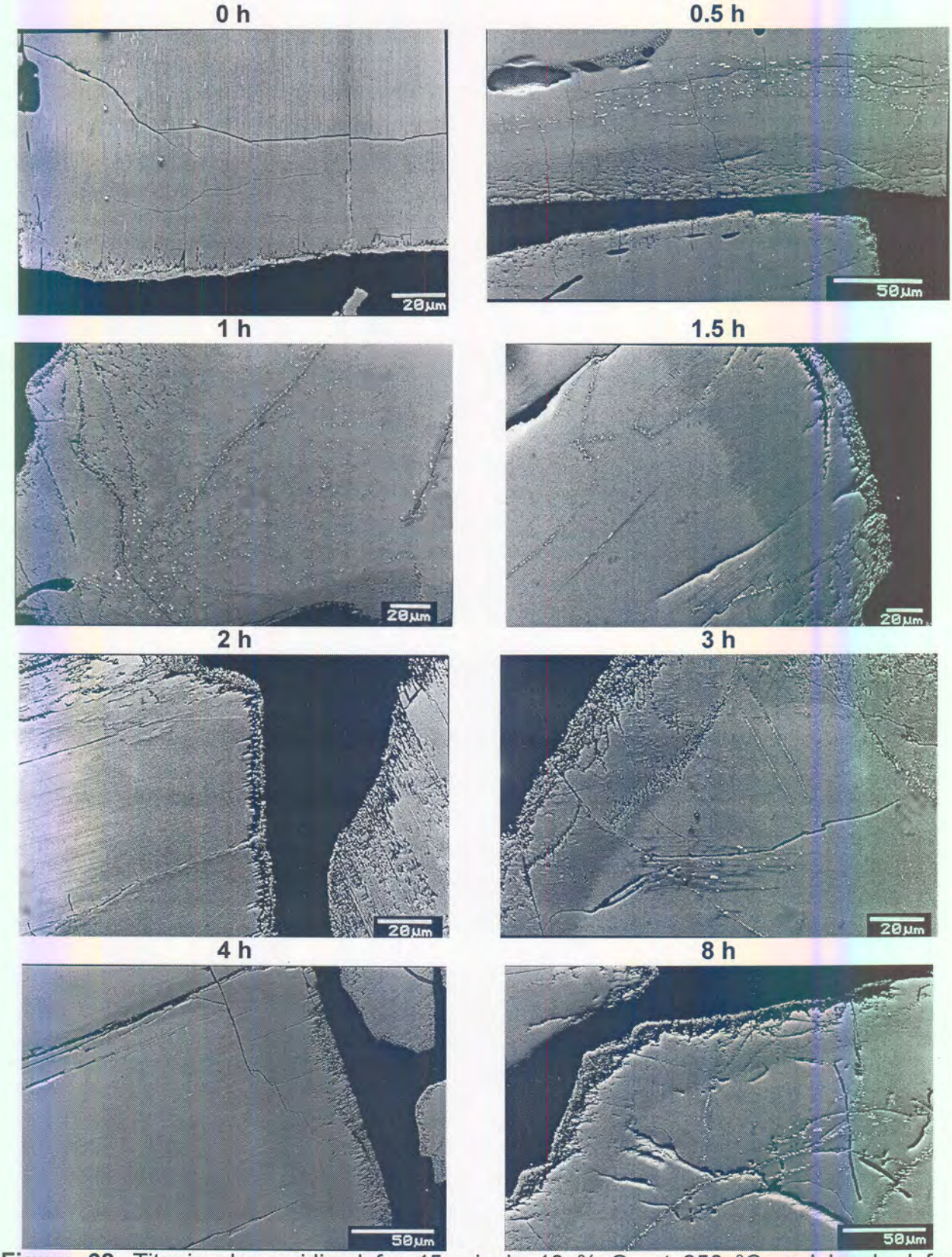

Figure 68. Titania slag oxidised for 45 min in 10 % O_2 at 850 °C and leached for different times under reducing conditions.

To provide information on the oxidation state of iron in the mantle zones two experiments were conducted. In the first experiment titania slag in the size range +710-850 µm was oxidised for 90 min at 850 °C in 10 % O_2 and leached for 8 h in boiling 20 % HCl without the addition of a reductant. The feed to the second experiment was roasted in the same manner as that for the first, but the slag was then subjected to a two stage leach procedure. Firstly the slag was leached for 1 h in boiling 20 % HCl with $SnCl_2$ added as a reductant to remove the iron-rich rims on the slag particles. Thereafter the slag was separated from the leach solution, washed and dried before it was leached again for 8 h in boiling 20 % HCl, without addition of $SnCl_2$. In the leaches where $SnCl_2$ was absent the speciation of iron in the leach solutions was determined by titration. The results of the experiments are listed in Appendix XV.

Figure 69 shows the speciation of iron in the leach solution of the slag where the iron-rich rims had not previously been removed. Initially iron goes into solution as Fe(III) and as leaching proceeds Fe(II) starts to appear along with Fe(III). This supports the proposed oxidation mechanism as follows: The Fe(III) that initially goes into solution is located on the outsides of the particles. With time the leach solution start to penetrate into the particles and Fe(II) goes into solution. Fe(III) continues to be a major component of the leach solution as the rate of Fe(III) dissolution is very slow and this shields the majority of the Fe(II) located beneath the surface of the particles.

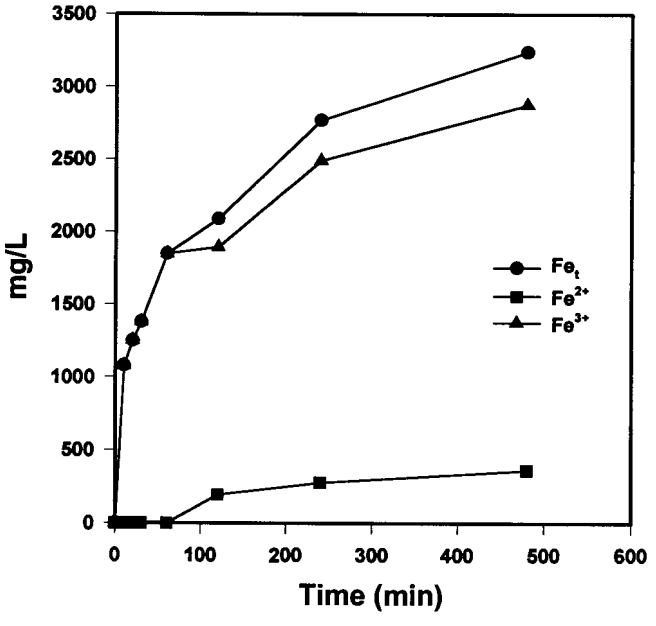

Figure 69. Iron speciation in solution during leaching of oxidised titania slag.

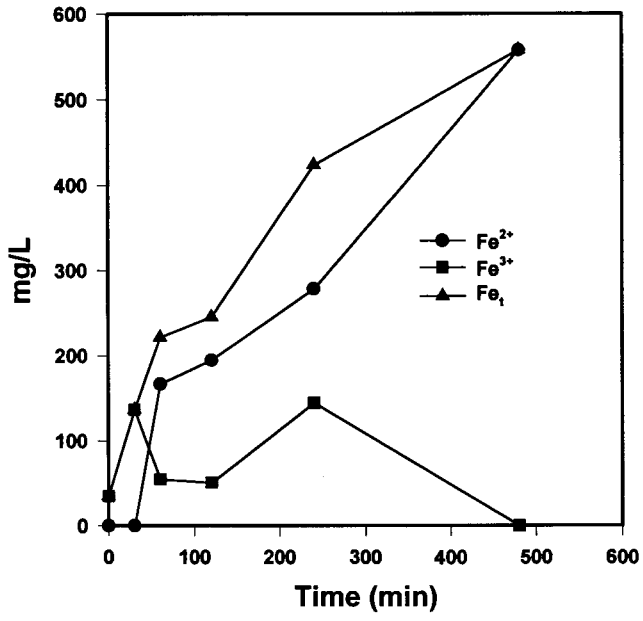

Figure 70. Iron speciation in solution during leaching of slag that was previously oxidised and reduction leached.

Figure 70 gives the speciation of iron in the leach solution of the slag where the iron-rich rims had previously been removed. Initially only Fe(III) is present in the leach solution, but soon the amount of Fe(III) in solution starts to decline and Fe(II) starts to appear. With extended leaching Fe(III) eventually disappears, while the amount of Fe(II) in solution continues to increase. This data supports the proposed oxidation mechanism as follows: The Fe(III) that initially goes into solution is a remnant of the iron-rich rims. With further leaching Fe(II) and Ti(III) comes into solution from the interiors of the particles. The Ti(III) in solution reduces the Fe(III) in solution until all the iron is present as Fe(II).

The results of these two experiments tentatively support the conclusion that iron in the enriched rim is present as Fe(III), but largely as Fe(II) deeper within the slag particles.

5.7.5 Investigation into influence of iron-rich rims on the mechanism of oxidation

The iron rich rims on the outsides of oxidised slag particles can lower the nucleation energy that is needed to precipitate additional M_2O_3. This would explain why migrating iron cations would preferentially precipitate at the iron-rich rim rather than at any other location. To test this hypothesis titania slag was oxidised at 850 °C in 10 % O_2 for 45 min and leached for 1 h under reducing conditions. After leaching the slag was washed and dried. The slag was then subjected to roasting for 2 h at 850 °C under three different atmospheres: air, argon and carbon monoxide. Micrographs of the different samples are presented in Figures 71 to 73. The phase compositions of the samples are given in Table 50.

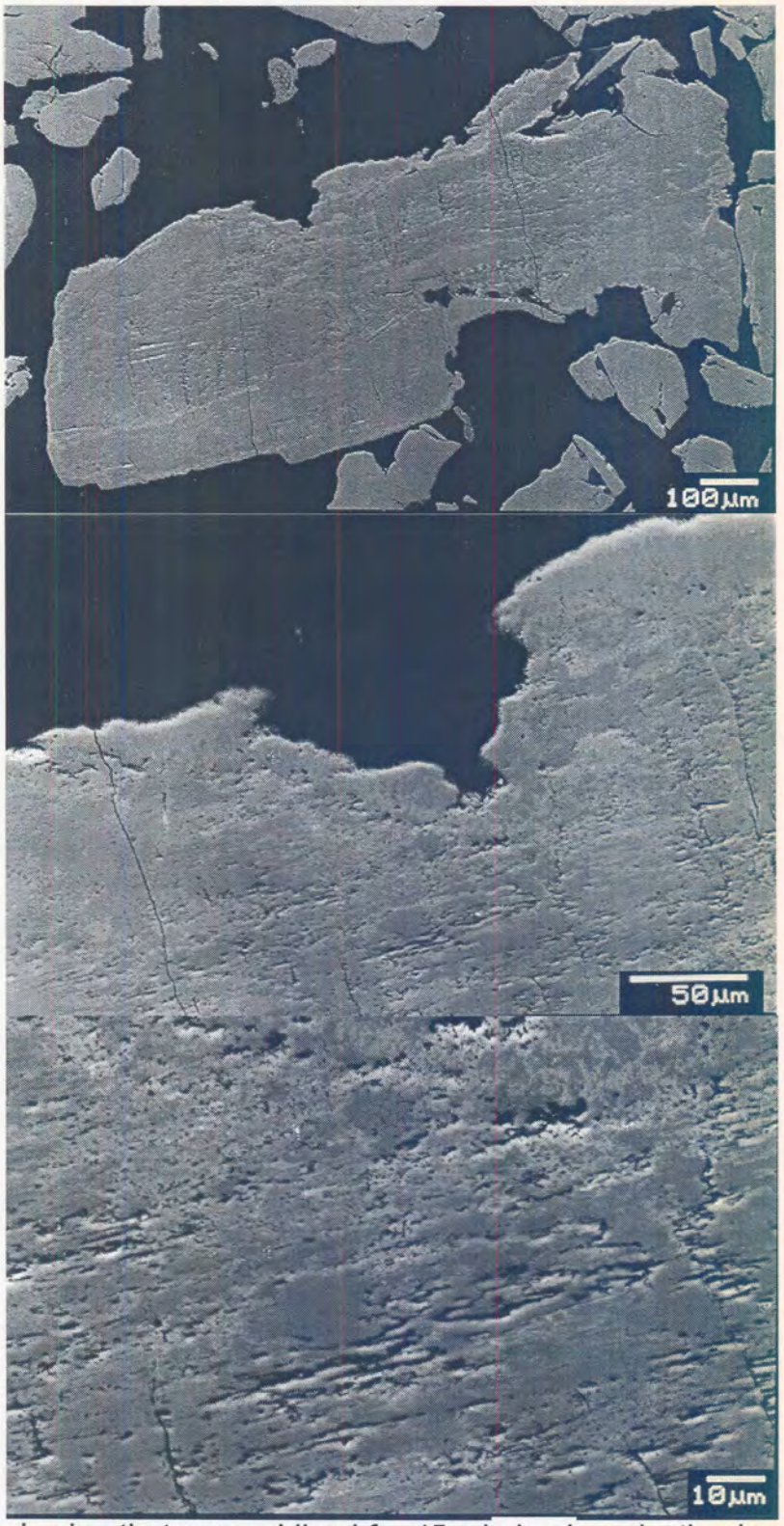

Figure 71. Titania slag that was oxidised for 45 min in air, reduction leached for 1 h and roasted again in air for 2 h at 850°C.

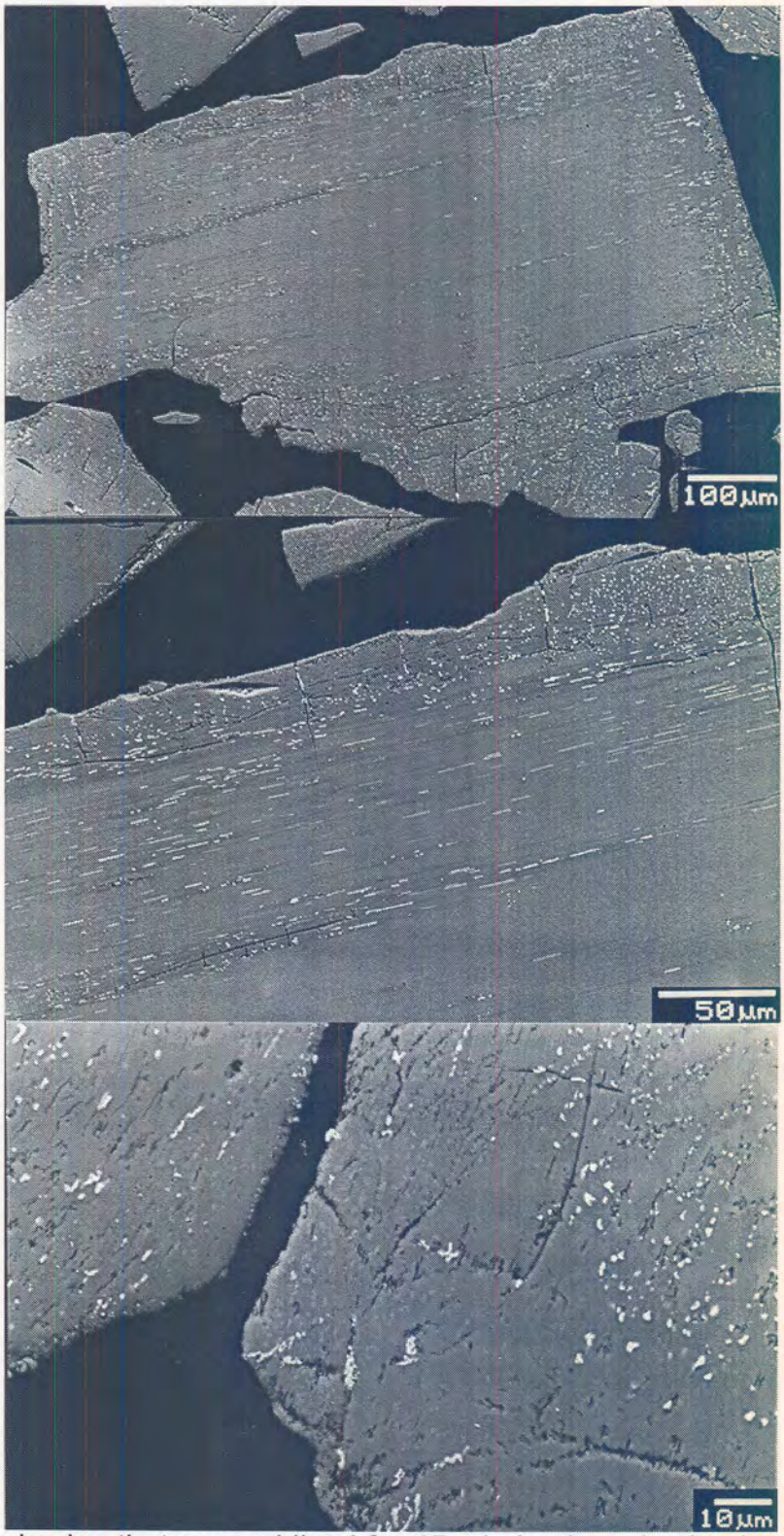

Figure 72. Titania slag that was oxidised for 45 min in air, reduction leached for 1 h and roasted again in argon for 2 h at 850°C.

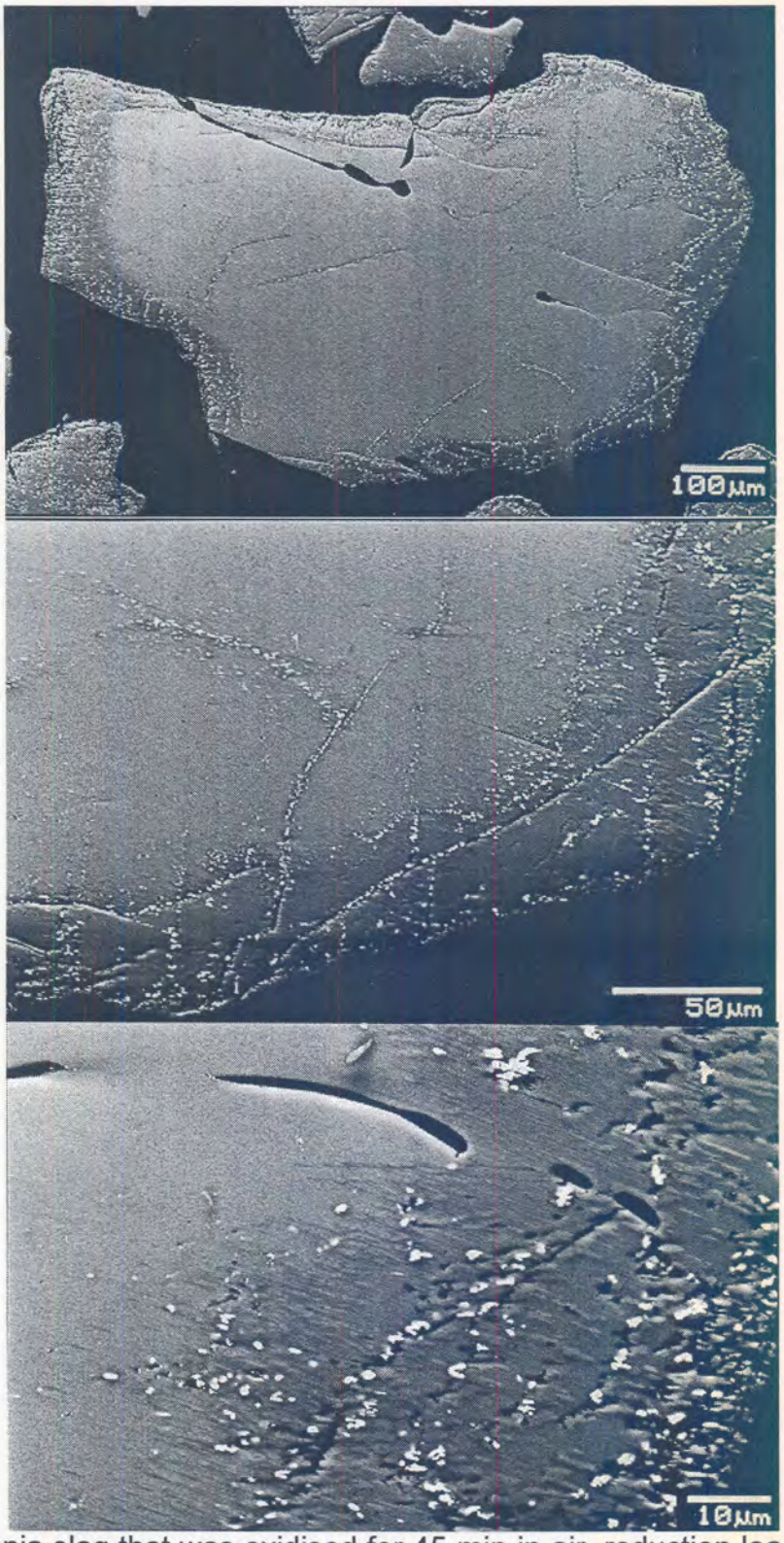

Figure 73. Titania slag that was oxidised for 45 min in air, reduction leached for 1 h and roasted again in carbon monoxide for 2 h at 850°C.

Table 50. Phase-chemical compositions as determined by XRD of oxidised and reduction leached titania slag after roasting in various atmospheres.

Description	Mineralogical composition		
	Main	Minor	Trace
Sample after reduction leach	Rutile, Anatase	FeTi-Oxide	-
Sample roasted in air	Rutile	Anatase, FeTi-Oxide	-
Sample roasted in argon	Rutile	Anatase, FeTi-Oxide	Iron, Ilmenite
Sample roasted in carbon monoxide	Anatase, FeTi-Oxide, Rutile	-	Iron

Legend: *Rutile - TiO_2; Anatase - TiO_2; FeTi-Oxide - M_3O_5-solid solution; Iron - Fe^o; Ilmenite - $FeTiO_3$*

Figure 71 shows micrographs of the leached slag after roasting in air. No unreacted cores were present. The outer rims of the particles were porous due to the previous leaching. Iron did not migrate to the outer surfaces of the slag particles. Instead iron-rich areas intimately mixed and intergrown with titania-rich areas could be observed throughout the particles. The XRD results (Table 50) indicate that the iron-rich phase was the M_3O_5 solid solution phase with rutile and anatase present as the titania-rich phases. This result shows that no iron migration towards the outer surfaces of the slag particles occurred in the absence of an iron-rich rim at the outer rims of the particles.

Figure 72 shows micrographs of the leached slag after roasting in argon. The slag particles were characterised by the occurrence of large unreacted M_3O_5-rich cores with a smooth and dense appearance. Fine-grained disseminated metallic iron precipitates were present and contained in the titania rich mantle zone. The XRD results (Table 50) show that small quantities of ilmenite were present in the particles. No iron migration occurred towards the previously leached outer rims of the slag particles. Metallic iron, rutile and ilmenite are the expected equilibrium phases for titania slag subjected to heat treatment in impure argon at 850°C (Figure 59). These phases were present towards the outer margins of the slag particles and it is assumed that if the slag was kept under these conditions for an optimum time period in order to reach equilibrium, the slag particles would consist entirely of these phases.

Figure 73 shows micrographs of the leached material after roasting in carbon monoxide. The slag particles were characterised by the occurrence of large M_3O_5 rich cores and well-defined TiO_2-rich mantle zones. Metallic iron was present mainly in the mantle zones. No iron migration occurred towards the outer rims of the slag particles. The XRD results (Table 50) indicated that the M_3O_5 solid solution phase increased to major phase after roasting. Anatase and rutile were also present as major phases in the slag. Metallic iron was present as a trace component. These phases correspond to those that are expected in titania slag in equilibrium with a carbon monoxide atmosphere at 850°C (Figure 59, Appendix XVI).

5.7.6 Investigation into the influence of higher roasting temperatures on the mechanism of oxidation

Chapters 3 and 4 showed that the optimum roasting temperature for the production of BTS is 850 °C. During oxidation at this temperature iron migrates from the insides of the slag particles towards the outsides where it is easily accessible during leaching.

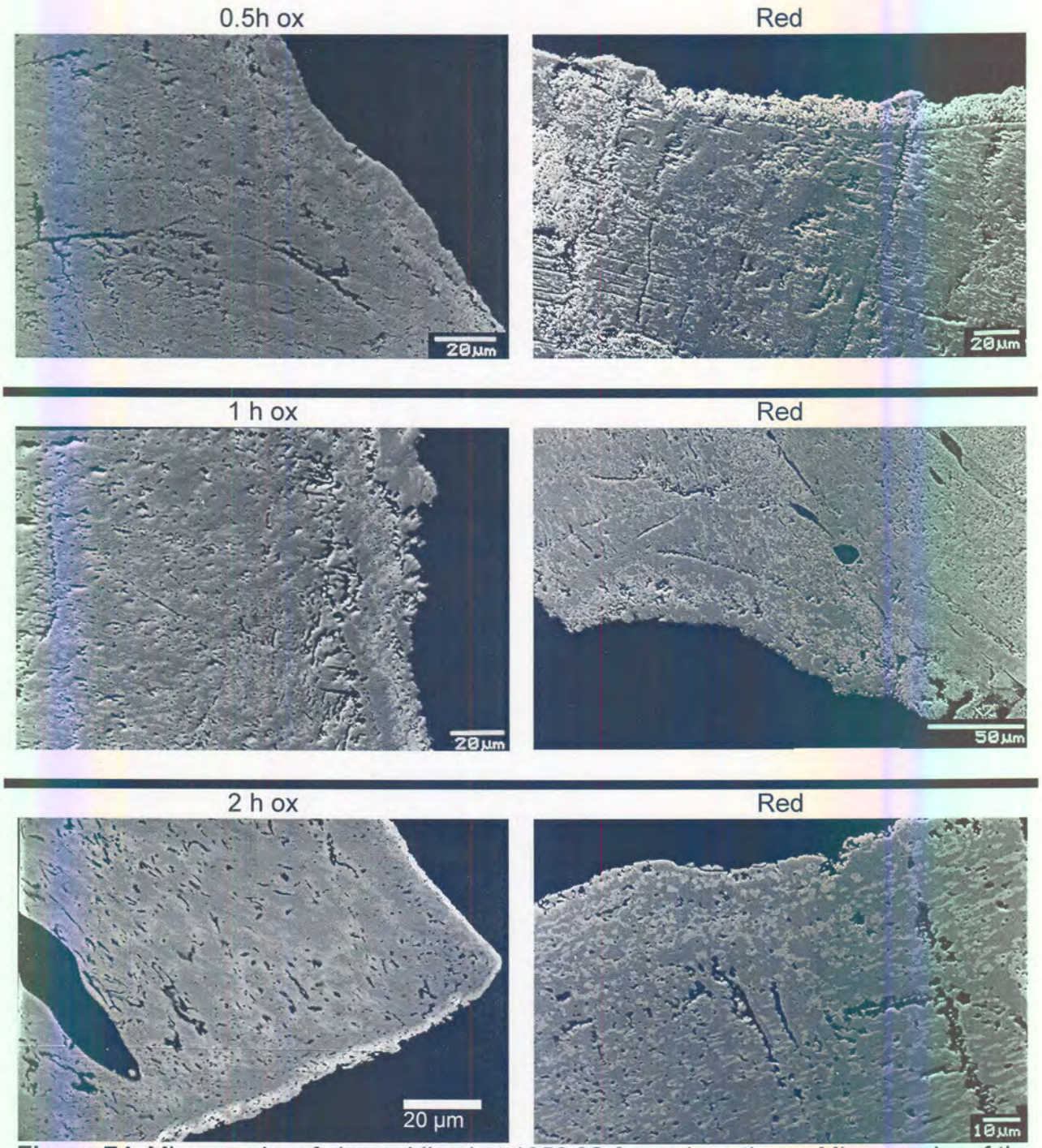

Figure 74. Micrographs of slag oxidised at 1050 °C for various times. Micrographs of the samples after reduction for 20 min at 850 °C are also shown.

Borowiec et al. (1994) patented a process for the upgrading of titania slag. Part of the process consists of oxidation above 1000 °C. They found that fast diffusion of iron and titanium occurred in the pseudobrookite phase during oxidation. This resulted in a large number of pores in the slag particles with the iron cations concentrated around these pores. Two different morphologies therefore seem to result when slag is oxidised at

higher and lower temperatures. It was decided to investigate this effect and it relevance to the mechanism of titania slag oxidation.

Slag was oxidised at 1050 °C for various times. Following this the slag was reduced at 850 °C for 20 min. Tables 51 and 52 give the phase compositions and the Mössbauer analysis of the samples respectively (The detailed results are shown in Appendix XVIII). Micrographs of the samples are presented in Figure 74.

Figure 74 shows titania slag roasted at 1050 °C for 0.5 h. It appeared to be much more porous compared to slag roasted at 850 °C (see Figure 63 as a comparison). Noticeable as well was the absence of unreacted cores. Iron migration occurred towards the outer rims of the slag particles as well as the margins of pores. Abundant rutile rich areas closely associated and in contact with iron-rich, titania poor areas were present, randomly distributed throughout the slag particles.

After a reductive roast abundant iron-rich precipitates were present randomly distributed throughout the particles. The XRD results (Table 51) suggest that the precipitates were ilmenite.

Table 51. Phase-chemical compositions of slag samples roasted at 1050 °C.

Description	Mineralogical composition		
	Main	Minor	Trace
Oxidised for ½ h	Rutile	-	FeTi-Oxide
Oxidised for ½ h & reduced for 20 min	Rutile	-	Ilmenite, FeTi-Oxide
Oxidised for 1 h	Rutile	-	FeTi-Oxide
Oxidised for 1 h & reduced for 20 min	Rutile	-	Ilmenite, FeTi-Oxide
Oxidised for 2 h	Rutile	-	FeTi-Oxide
Oxidised for 2 h and reduced for 20 min	Rutile	-	Ilmenite, FeTi-Oxide

Legend : Rutile - TiO_2; Ilmenite - $FeTiO_3$; FeTi-Oxide -M_3O_5-solid solution

The Mössbauer results (Table 52, see APPENDIX XVIII for the detailed results) show that all the Fe (II) in the as-cast slag was oxidised to Fe(III) within 0.5 h during oxidation at 1050 °C. After 0.5 h of oxidation most of the iron was present in the Fe_2TiO_5 phase, but some of the iron was also present in a hematite phase. The hematite phase disappeared as the oxidation time increased. After reduction all the samples contained iron in the Fe (III) and the Fe(II) oxidation states. Iron in the Fe(III) state was contained in the unconverted Fe_2TiO_5 phase, while iron in the Fe(II) state was distributed between predominantly ilmenite along with some M_3O_5.

Table 52. Mössbauer analysis of slag samples oxidised at 1050 °C and reduced at 850 °C.

PFE	Description	% Abundance	Attribution
3065	Oxidised for ½ h	84 16	Fe_2TiO_5 Hematite-like
3071	Oxidised for ½ h & reduced for 20 min	21 64 15	Fe_2TiO_5 Ilmenite-like $FeTi_2O_5$
3066	Oxidised for 1 h	100	Fe_2TiO_5
3072	Oxidised for 1 h & reduced for 20 min	20 65 15	Fe_2TiO_5 Ilmenite-like $FeTi_2O_5$
3067	Oxidised for 2 h	100	Fe_2TiO_5
3073	Oxidised for 2 h and reduced for 20 min	21 69 10	Fe_2TiO_5 Ilmenite-like $FeTi_2O_5$

The samples oxidised at 1050 °C were submitted for WDS line chemical analysis through some of the particles. The aim was to compare these results with that of slag particles roasted at 850 °C (Chapter 4). The results are presented in Figures 75 and 76.

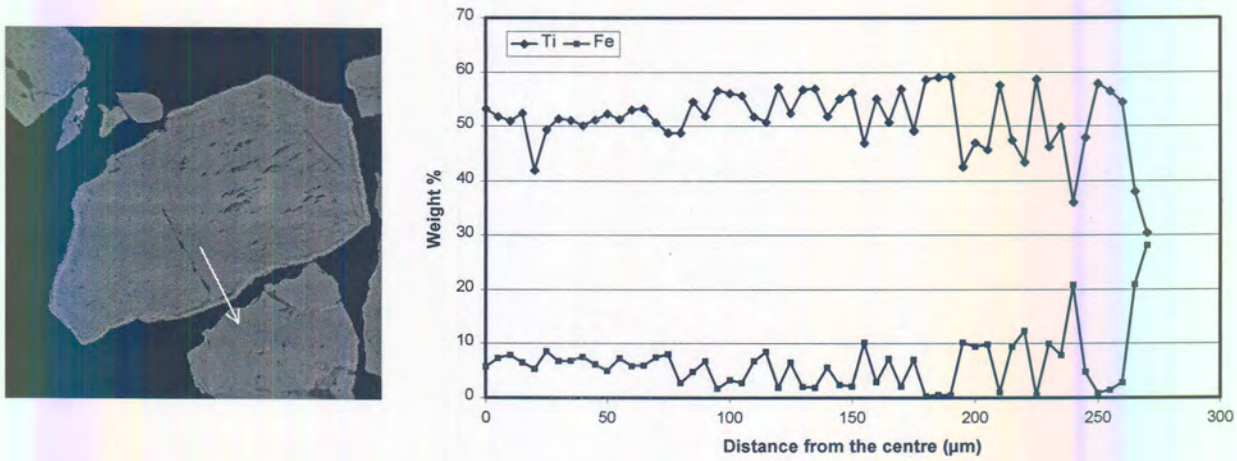

Figure 75. WDS Line chemical analysis through a particle of standard titania slag that was oxidised at 1050 °C for 30 min in 10 % O_2.

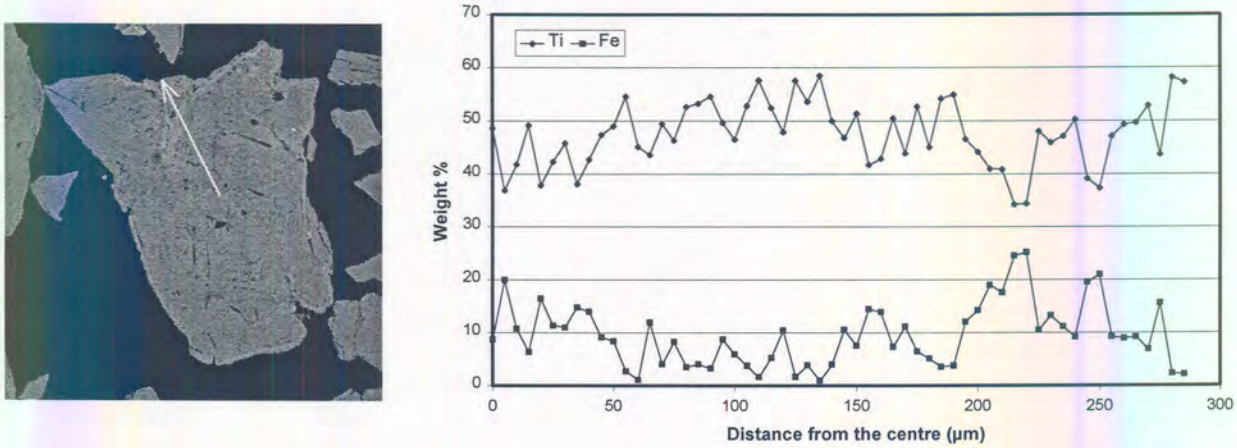

Figure 76. WDS Line chemical analysis through a particle of standard titania slag that was oxidised at 1050 °C for 60 min in 10 % O_2.

The results presented in Figures 75 and 76 show that unreacted cores were present in some particles after 30 min of oxidation, but after 60 min no cores could be observed. The line chemical analyses in the reacted zones of the particles showed a large variation in titanium and iron concentration with position. This behaviour can be related to the morphology of the particles. All of the particles were very porous and the large variation in iron and titanium concentrations suggests that iron migration occurred to the margins of the pores. This resulted in titanium rich areas intermingled with iron rich areas.

The morphology observed in the samples oxidised at 1050 °C was similar to that described by Borowiec et al. (1996). The difference in morphology between samples oxidised at 850 °C and 1050 °C can be explained by the proposed titania slag oxidation mechanism. According to the thermodynamic considerations discussed in paragraph 5.3.2 the stability area of hematite decreases with increasing temperature. There is consequently a much smaller amount of M_2O_3 that precipitates at higher temperatures (See Appendix XVII). The nucleation energy that is needed to for ferric pseudobrookite is probably much less than that needed to precipitate hematite. Iron-rich pseudobrookite consequently precipitates through the slag particles at higher roasting temperatures.

5.7.7 Investigation into the influence of interrupted roasting on the mechanism of oxidation

Two experiments were conducted to test whether an interruption in the roasting process changes the mechanism of oxidation. The first experiment was performed by subjecting titania slag to an oxidative roast in air for 30 min at 850 °C whereafter the slag was cooled down to room temperature and oxidised again in air for 2 h at 850 °C. For the second experiment titania slag was subjected to an oxidative roast in air for 30 min at 850 °C, cooled down to room temperature and subjected to a second oxidative roast in air for 2 h at 1050 °C. Micrographs of the two samples are shown in Figures 77 and 78. The phase chemical compositions of the samples are given in Table 53.

Table 53. Phase-chemical composition as determined by XRD-analysis of the samples subjected to interrupted roasting.

Sample No.	Roast procedure	Mineralogical composition		
		Main	Minor	Trace
A524-57	1st Roast - 850 °C, 30 min, air 2nd Roast – 850 °C, 2 h, air	Anatase; Rutile	FeTi-Oxide	-
A524-58	1st Roast – 850 °C, 30 min, air 2nd Roast – 1050 °C, 2 h, air	Rutile	FeTi-Oxide	-
A524-59	1st Roast – 850 °C; 30 min, air 2nd Roast – 1050 °C; 2 h; air 3d Roast – 850 °C; 20 min; 100 % CO	Rutile	-	FeTi-Oxide; Ilmenite

Legend : Rutile - TiO_2; FeTi-Oxide – M_3O_5 solid solution ; Anatase – TiO_2

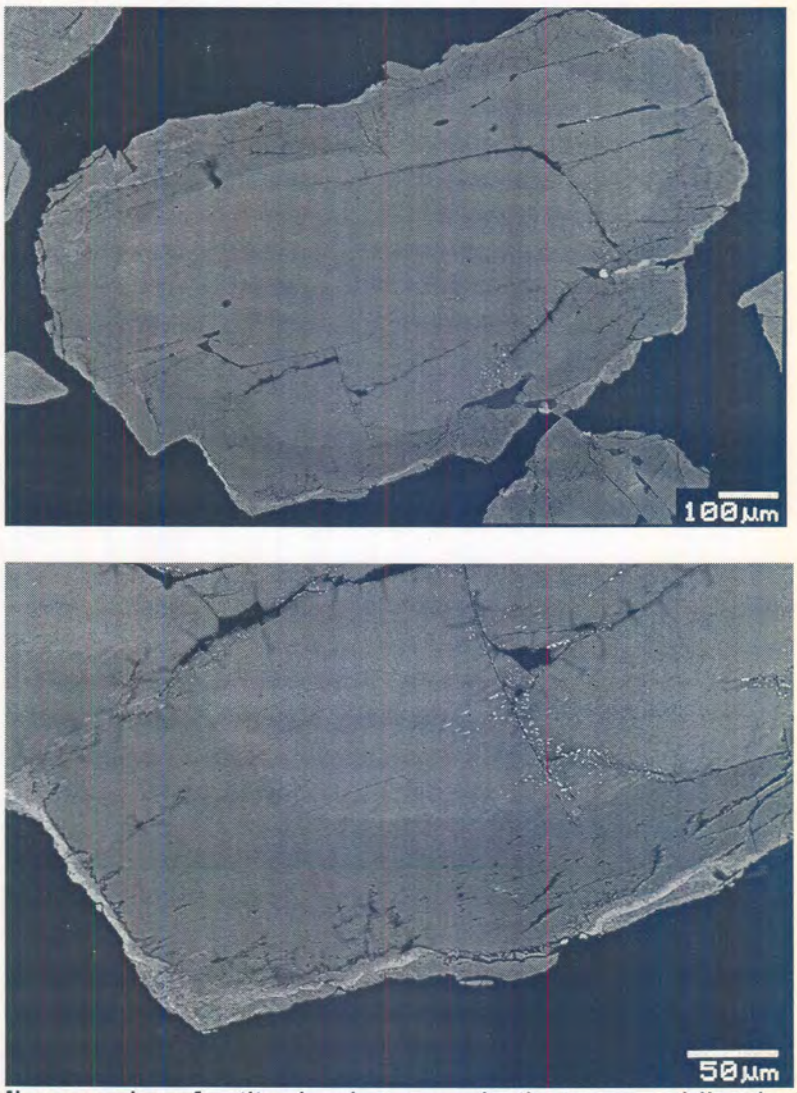

Figure 77. Micrographs of a titania slag sample that was oxidised at 850 °C for 30 min, then cooled to room temperature and oxidised again at 850 °C for 2 h.

The sample subjected to an oxidative roast in air at 850 °C for 30 min. and roasted again in air for 2 h at 850 °C consisted predominantly of anatase and rutile with lesser amounts of the M_3O_5 solid solution phase. Optically the slag particles looked similar to slag samples that were roasted without interruption (Figure 77). The particles had a zoned texture and iron migration occurred towards the outer margins of the individual slag particles. Oxidation occurred along cracks cutting through the unreacted M_3O_5-rich cores with the crystallisation of rutile associated with the occurrence of fine metallic iron "blebs" and precipitates. An interruption in the normal roast procedure therefore did not change the oxidation mechanism.

The titania slag sample subjected to an oxidative roast in air at 850 °C for 30 min and roasted again in air at 1050 °C for 2 h consisted primarily of rutile with minor amounts of the M_3O_5-solid solution phase. No anatase was observed by XRD-analysis. Optically the slag particles seemed to be in general completely oxidised and transformed to rutile (Figure 78). Only a few of the coarser-grained slag particles displayed small oxidised M_3O_5-rich cores. Iron migration occurred towards the outer margins of the slag particles with the majority of slag particles displaying well-defined iron enriched outer rims. A thin relatively fragile rutile-rich layer seemed however to have formed beyond these iron-enriched rims. The mantle zones of the slag particles appeared to be very porous. The outer margins of the individual pores were characterised by iron enrichment as iron migration occurred towards the outer margins of the pores. The cores of the particle had in general a relatively dense appearance.

Some of the slag particles displayed a well-defined crystalline texture and seemed to be partially to completely recrystallised during the roasting procedure. The recrystallised slag particles appeared to be much more porous compared to the slightly denser appearance of the remainder of the slag particles. The recrystallised slag particles consisted primarily of densely packed, fine-grained, rounded to slightly elongated, rutile crystals whereas in other particles crystallisation seems to be uncompleted with coarse-grained rutile "blebs" and precipitates as well as needles and laths "embedded" in the oxidised M_3O_5 rich matrix (Figure 79). These recrystallised particles displayed well-defined iron enriched outer margins. These iron-rich outer margins displayed a crystalline nature consisting of densely packed and interwoven fine-grained tabular-, needle- and lath-like crystals. The slag sample was furthermore characterised by the occurrence of several sintered slag particles as sintering occurred between the iron-enriched outer rims of the individual slag particles (Figure 80).

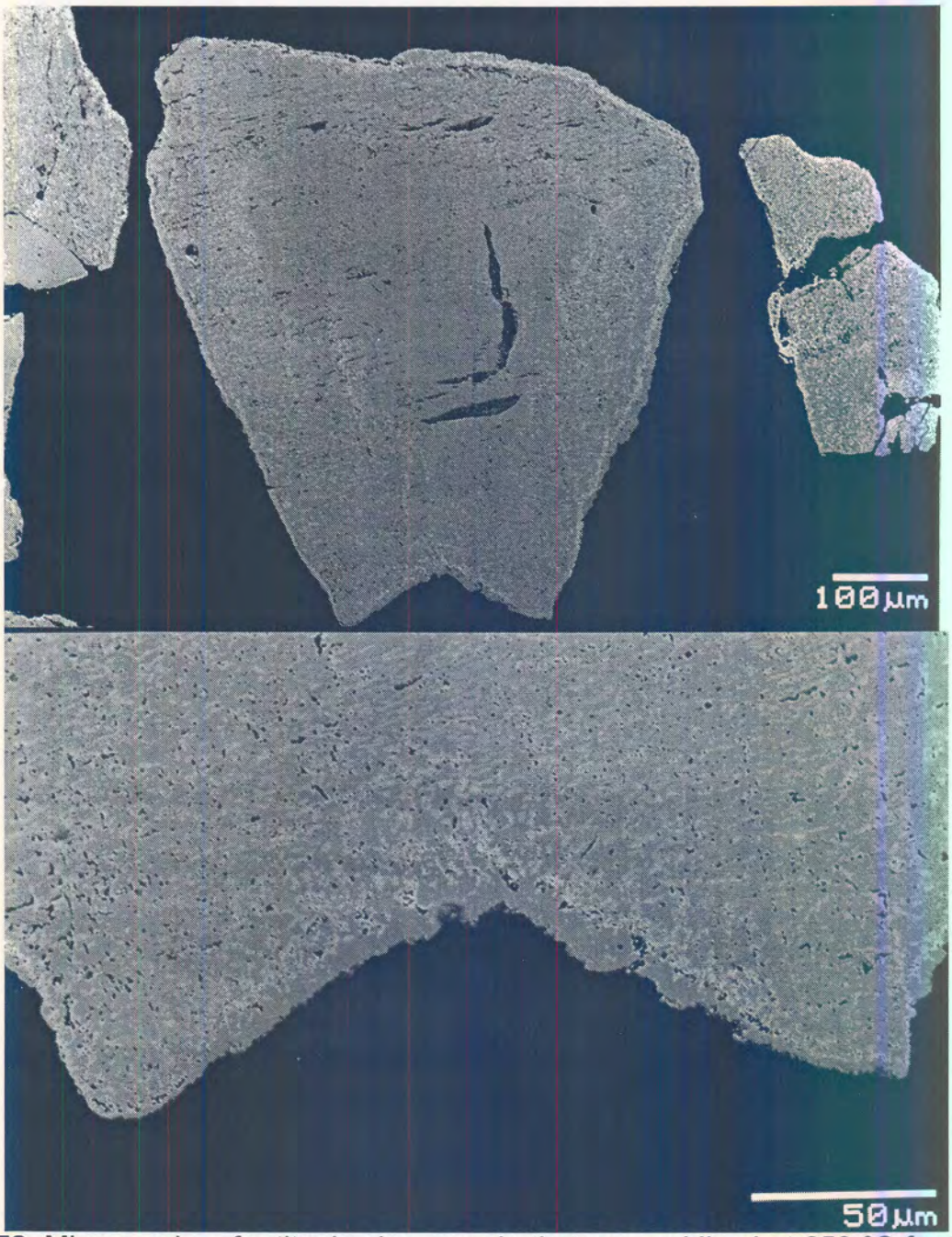

Figure 78. Micrographs of a titania slag sample that was oxidised at 850 °C for 30 min, then cooled to room temperature and oxidised again at 1050 °C for 2 h.

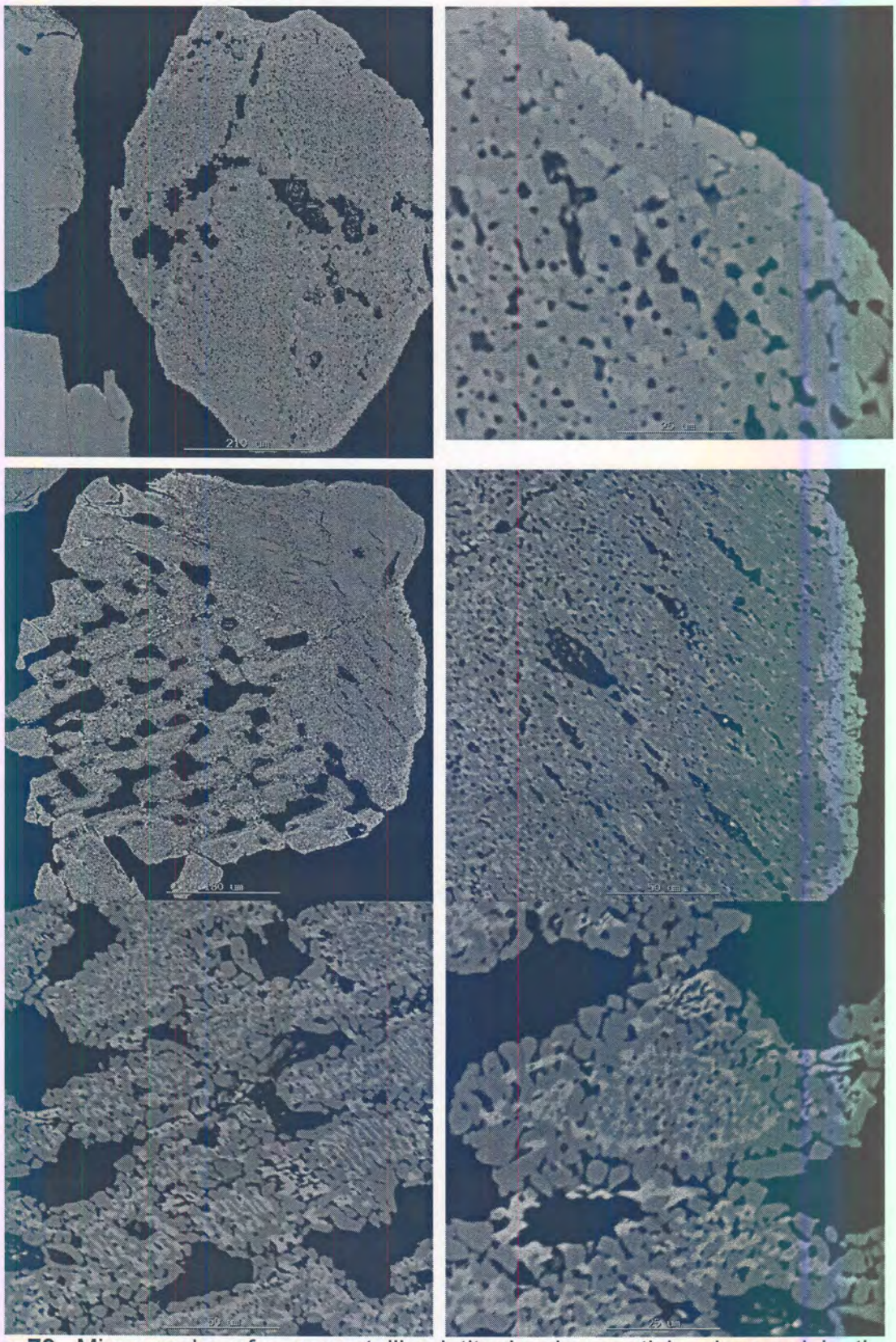

Figure 79. Micrographs of a recrystallised titania slag particle observed in the slag sample that was oxidised at 850 °C for 30 min, then cooled to room temperature and oxidised again at 1050 °C for 2 h

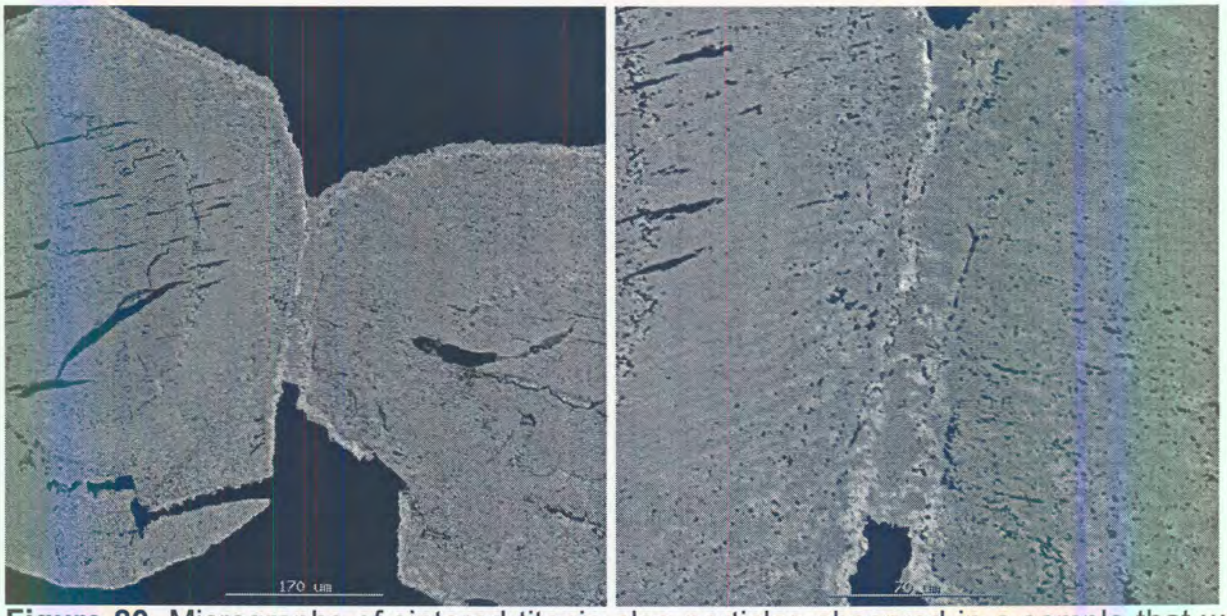

Figure 80. Micrographs of sintered titania slag particles observed in a sample that was oxidised at 850 °C for 30 min, then cooled to room temperature and oxidised again at 1050 °C for 2 h.

An explanation of the morphology observed in the sample oxidised at 850 °C for 30 min and then oxidised further at 1050 °C can be attempted by using the proposed oxidation mechanism. During oxidation at 850 °C iron migrates to the outside rims of the particles where it precipitates as M_2O_3 and M_3O_5. This results in the formation of an iron-rich rim on the outsides of the particles. When the partially oxidised sample is then further oxidised at 1050 °C a different morphology result. This is as a result of the instability of M_2O_3 at higher temperatures. The iron now preferentially precipitates as M_3O_5 which is potentially much easier to nucleate. The hematite that previously precipitated on the outsides of the particles now also converts to pseudobrookite. The exothermic reaction heat that is generated during oxidation can explain the sintering that was observed between some of the particles. This heat in conjunction with the high furnace temperature resulted in the sintering. The recrystallisation that was observed in about a third of the particles cannot be explained by the proposed oxidation mechanism. This may have occurred as a result of the high temperature and the resulting high reaction rates that allowed the slag sample to move rapidly towards thermodynamic equilibrium.

5.8 Quantitative WDS analyses of selected phases in oxidised slag

The composition of selected phases in oxidised titania slag were determined quantitatively by SEM-WDS. A summary of the data presented in Chapter 4, Figure 28 is shown in Table 54. These phases include TiO_2 and the solid solution phases M_3O_5 and M_2O_3. In the instances where M_3O_5 and M_2O_3 were identified the cation to oxygen stoichiometric ration was forced to be equal to either 3:5 or 2:3 whereby the relative amounts of Ti(IV), Ti(III), Fe(II) and Fe(III) in the M_3O_5 and M_2O_3 phases were calculated.

Table 54. Quantitative WDS analyses of selected phases in oxidised slag.

Locations	Al_2O_3%	MnO%	MgO%	TiO_2%	FeO%	Total%	Stoichiometry
Core	1.29	1.42	1.35	91.69	9.85	105.6	$Ti^{4+}_{1.42}Ti^{3+}_{1.11}Fe^{2+}_{0.3}Al^{3+}_{0.06}Mg^{2+}_{0.07}Mn^{2+}_{0.04}O_5$
Mantle	0.71	0.49	0.51	96.15	1.85	99.71	$Ti^{4+}_{0.95}Fe^{2+}_{0.02}Al^{3+}_{0.01}Mg^{2+}_{0.01}Mn^{2+}_{0.01}O_2$
Rim	3.68	0.41	1.25	43.96	48.45	97.75	$Ti^{4+}_{0.82}Fe^{2+}_{0.77}Fe^{3+}_{0.24}Al^{3+}_{0.11}Mg^{2+}_{0.05}Mn^{2+}_{0.01}O_3$

Using the data in Table 54 a balanced chemical reaction can be written for the oxidation of titania slag:

$$Ti^{4+}_{1.42}Ti^{3+}_{1.11}Fe^{2+}_{0.3}Al^{3+}_{0.06}Mg^{2+}_{0.07}Mn^{2+}_{0.04}O_5 + 0.48O_2 \rightarrow 0.3Fe^{2+}_{0.77}Fe^{3+}_{0.24}Al^{3+}_{0.02}Mg^{2+}_{0.02}Mn^{2+}_{0.01}O_3 + 2.53TiO_2$$

5.9 Conclusions

An oxidation mechanism for titania slag was proposed: The mechanism is based on the phases that form during oxidation. At lower roasting temperatures rutile, M_2O_3 and M_3O_5 form in the slag. The nucleation energy that is needed for the precipitation of individual M_2O_3 crystals is probably much higher than that needed to precipitate individual rutile and M_3O_5 crystals, because the crystal structure of M_2O_3 differs radically from M_3O_5. This results in the migration of iron to the outside surface of the slag particles where less nucleation energy is needed to precipitate M_2O_3 on the existing free surfaces. At higher roasting temperatures the stability of M_2O_3 declines and the iron precipitates as M_3O_5 throughout the particles.
This mechanism was tentatively confirmed through selected experiments:

- It was shown that oxygen is required for iron migration to occur;
- Particle size measurements of oxidised slag as well as an experiment conducted with a gold marker on the slag confirmed that the particle size of the slag increases as the iron migrates to the outside surfaces of the particles;
- The role of the iron-rich rim, as a site where low nucleation energy is required for the continued precipitation of M_2O_3, was confirmed when the iron-rich rim was removed with reductive leaching. Under these conditions iron did not continue to migrate to the outside surfaces of the particles, but precipitated locally;
- Roasting at temperatures in excess of 1000°C changed the morphology of the oxidised slag and iron migration no longer occurred to the outside surfaces of the particles. This may be related to the instability of M_2O_3 at higher temperatures and;
- An interruption in the oxidation process did not change the morphology of the oxidised slag, but partial oxidation at lower temperatures followed by oxidation at temperatures in excess of 1000°C did change the morphology of the slag drastically; Iron stopped migrating to the outside surfaces of the particles and rather precipitated locally.

To take advantage of iron migration the oxidation conditions need to be chosen very carefully as this phenomenon is not dependent of equilibrium behaviour, but rather on kinetic behaviour of the system.

SUMMARY

Phase 1 of the process development for the production of beneficiated titania slag was conducted with a coal fired fluid bed. Based on the results from this investigation the following optimum processing conditions were recommended:

- Oxidation: 3 h at 850°C
- Reduction: 30 min at 800°C
- Leaching: 12 h with 20% HCl at 20% excess

It was also found that the most important process parameters were roasting temperature and the chemical composition of the slag. The highest TiO_2 content achieved was 94%.

Phase 2 of the process development was conducted under more stringent roasting conditions, where the gas atmosphere in the reactor was regulated with a gas mixing system. Based on the results from this investigation the following optimum process conditions are recommended:

- Oxidation: 1.5 h at 850° in 8% O_2
- Reduction: 10 min at 850°C in 100% CO
- Leaching 12 h with 20 % HCl

As part of the process development the phase changes that occur were characterised; during oxidation the $FeTi_2O_5$-Ti_2O_3 (ferrous M_3O_5) phase that is present in the as-cast slag is oxidised to rutile or anatase, M_2O_3 and Fe_2TiO_5-$FeTi_2O_5$ (ferric M_3O_5). During reduction the M_2O_3 and ferric M_3O_5 phases are converted to ilmenite. The ilmenite phase as well as the residual M_3O_5 phase in the slag that contains most of the impurities is removed during the leaching stage. The highest TiO_2 content that was achieved was 97.5%.

An important additional benefit that occurs during oxidation is the migration of iron to the outsides of the slag particles where it is easily accessible during leaching. The mechanism whereby this occurs was investigated and it was postulated that the iron migration is linked to high nucleation energy that is needed for the formation of the separate M_2O_3 crystals. The iron seems to preferentially precipitate at the free surface that is created at the iron-rich rim. This hypothesis was tentatively confirmed through selected experiments.

The following issues remain unresolved:

- The effect of impurities such as Ca and Mg on the mechanism of oxidation;
- A detailed investigation of the crystal changes that occur during oxidation;
- An in depth investigation into the leach behaviour of roasted slag and;
- A larger scale demonstration of the BTS process.

REFERENCES

- Abuluwefa, H.T., Guthrie, R. and Ajersch, F. 1997. Oxidation of low carbon steel in multicomponent gases: Part I. Reaction mechanism during isothermal oxidation. *Met. Trans. A*, 28A, pp. 1633-1641.
- Akimoto, T., Kinoshita, H. and Furuta, T. 1984. Electron probe microanalysis study on processes of low-temperature oxidation of titanomagnetite. *Earth and Planetary science Letter*, 71, pp. 263-278.
- Amorelli, A., Evans, J.C. and Rowlands, C.C. 1987. An electron spin resonance study of rutile and anatase titanium dioxide polycrystalline powders treated with transition metals ions. *J. Chem. Soc., Faraday Trans.*, 12, pp. 3541-3548.
- Bickley, R.I., Gonzalez-Carreño, T., Gonzalez-Elipé, A.R., Munuera, G. and Palmisano, L. 1994. Characterisation of iron/titanium oxide photocatalysts. *J. Chem. Soc., Faraday Trans.*, 90(15), pp. 2257-2264.
- Bickely, R.I., Gonzalez-Carreño, T. and Palmisano, L. 1991. A study of the interaction between iron(III)oxide and titanium(IV)oxide at elevated temperatures. *Materials Chemistry and Physics*, 29, pp. 475-487.
- Briggs, R.A. and Sacco, A. 1993. The oxidation of ilmenite and its relationship to the FeO-Fe_2O_3-TiO_2 phase diagram at 1073 and 1140 K. *Met. Trans. A*, 24A, June, pp. 1257-1264.
- Borowiec, K., Grau, A.E., Gueguin, M. and Turgeon, J.F. 1996. Method to upgrade titania slag and resulting product. *South African Pat. 96/9772*.
- Borowiec, K., Grau, A.E., Gueguin, M. and Turgeon, J.F. 1998. Method to upgrade titania slag and resulting product. *US Pat. 5,830,420,* 3 Nov.
- Borowiec, K. and Rosenqvist, T. 1981. Phase relations and oxidation studies in the system Fe-Fe_2O_3-TiO_2 at 700-1100°C. *Scand. J. Metall.*, 20, pp. 91-119.
- Borowiec, K., Rosenqvist, T., Tuset, J.Kr. and Ulvensøen, J.H. 1987. Synthetic rutile from titaniferous slags by a pyrometallurgical route. Pyrometallurgy '87,IMM, London (UK), pp.91-119.
- Bull, D.S. 1992. Titanium dioxide pigments by the chloride process. *Paint and Resin*, January/February, pp. 15-19.
- Chiang, Y.M., Henriksen, A.F. and Kingery, W.D. 1981. Characterisation of grain-boundary segregation in MgO. *J. Am. Ceram. Soc.*, 64(7), pp. 385-389.
- Cook, R.F. and Schrott, A.G. 1988. Calcium segregation to grain boundaries in alumina. *J. Am. Ceram. Soc.*, 71(1), pp. 50-58.
- Doan, P.H. 1996. Upgraded slag (UGS): implications for TiO_2 feedstock supply. Proceedings of *12th Industrial Minerals Int. Congress*, pp. 71-76.
- Elger G.W. and Holmes R.A. 1982. Purifying titanium-bearing slag by promoted sulfation. *U.S. Pat 4,362,557*, 7 Dec.
- Elger, G.W., Kirby, D.E., Rhoads, S.C. and Stickney, W.A. 1974. *Synthesis of rutile from domestic ilmenites.* US Bureau of Mines Report of Investigation 7985, pp. 19.
- Ericksson, G. and Pelton, A.D. 1996. Measurement and thermodynamic evaluation of phase equilibria in the Fe-Ti-O system. Ber. Bunsenges. Phys. Chem., 100(11), pp. 1839-1849.
- FACT thermodynamic database, http://www.crct.polymtl.ca/fact/fact.htm
- Fisher, J.R. 1997. Developments in the TiO_2 pigment industry which will drive demand for TiO_2 mineral feedstocks. In: *Heavy Minerals 1997*. Ed. R.E. Robinson, SAIMM, Johannesburg (South Africa), pp. 207-218.
- Gambogi, J. 1991. Minerals Yearbook: Titanium. *Annual Report: United States Department of the Interior, Bureau of Mines.*
- Gambogi, J. 1998. Minerals Yearbook: Titanium. *Annual Report: United States Geological Survey.*
- Gueguin, M. 1986. Process of producing synthetic rutile from titaniferous product having a high reduced titanium oxide content. *US Pat. 4,629,607*, 16 Dec.
- Gueguin, M. 1990. Method of preparing a synthetic rutile from a titaniferous slag containing magnesium values. *US Pat. 4,933,153*, 12 Jun.
- Gueguin, M. 1991. Method of preparing a synthetic rutile from a titaniferous slag containing alkaline earth metals. *US Pat. 5,389,355*, 14 Feb.
- Gueguin, M. 1995. Method of preparing a synthetic rutile from a titaniferous slag containing magnesium values. *US Pat. 5,063,032*, 5 Nov.
- Gueguin, M. and Grau, A.E. 1989. Upgrading of titania slags by fluidized-bed selective

vol 3, Editor D. Rumble III, Mir a, Chelsea, Michigan, pp. Hg1-Hg98.

- Hollit, M.J., O'Brien, B.A. and Grey, I.E. 1995. Production of synthetic rutile. *US Pat. 5,427,749*, 27 Jun.
- Holman, J.P. 1976. *Heat Transfer*. McGraw-Hill Kogakusha Ltd., Tokyo, pp. 503.
- Iscor Heavy Minerals Brochure. 1997. Distributed during the Heavy Minerals Congress.
- Jarish, B. 1977. Upgrading Sorelslag for production of synthetic rutile. *US Pat. 4,038,363*, 26 Jul.
- Kingery, W.D. (1984) Segregation phenomena at surface and at grain boundaries in oxides and carbides. *Solid state ionics*, 12, pp. 299-307.
- Kubaschewski, O., Alcock, C.B. and Spencer, P.J. 1993. *Materials Thermochemistry*, 6th edition. Pregamon, Oxford.
- Kunii, D. and Levenspiel, O. 1977. *Fluidization Engineering*. Robert E. Kriegler Publishing Co., Huntington, N.Y.
- Leddy, J.J. and Schechter, D.L. 1962. Pressure leaching of titaniferous material. *US Pat. 3,060,002*, 23 Oct.
- Lindsley, D.H. 1976. Experimental studies of oxide minerals. *In Reviews in Mineralogy, vol.3*, Editor D. Rumble III, Mineralogical Society of America, Chelsea, Michigan, pp. L61-L84.
- Lurie, J. 1987. *South African geology*, Lexicon.
- Lynd, L.E., Sigurdson, H., North, C.H. and Anderson, W.W. 1954. Characteristics of titaniferous concentrates. *Trans. AIME*, Aug, pp. 817-824.
- Minkler, W.W. and Baroch, E.F. 1981. The production of titanium, zirconium and hafnium. Proceedings of TMS-AIME USA-China Bilateral Conference: *Metallurgical Treatises* (edited by J.K. Tien and J.F. Elliot), pp. 171-185.
- Nafziger, R.H. and Elger, G.W. 1987. Preparation of titanium feedstock from Minnesota ilmenite by smelting and sulfation-leaching. *US Bureau of Mines RI9065*.
- Nicol, M.J. 1983. The non-oxidative leaching of oxides and sulphides: an electrochemical approach. *In Hydrometallurgy: Research, Development and Plant Practice*, Editors K. Osseo-Asare and J.D. Miller, SME-AIME, Warrendale PA (USA), pp. 177-195.
- Nobile, A. and Davis, M.W. 1989. Importance of the anatase-rutile phase transition and titania grain enlargement in the strong metal-support interaction phenomenon in Fe/TiO_2 catalysts. *J. Catalysis*, 116, pp. 383-398.
- Oden, L.L., Sumner, D.H., Howe, J. 1973. Studies on recovering rutile from titanium-enriched-high iron-smelter slag. *U.S. Bureau of Mines Report of Investigation 7742*, p. 10.
- O'Reilly, W. and Banerjee, S.K. 1966. Oxidation of titanomagnetites and self reversal. *Nature*, 211, pp. 26-28.
- Perry, R.H. and Green, D. (eds.). 1984. *Perry's chemical engineers' handbook*. Sixth edition. McGraw-Hill Book Company, Tokyo.
- Pint, B.A., Garratt-Reed, A.J. and Hobbs, L.W. 1998. Possible role of oxygen potential gradient in enhancing diffusion of foreign ions on α-Al_2O_3 grain boundaries. *J. Am. Ceram. Soc.*, 81(2), pp. 305-314.
- Rao, D.B. and Rigaud, M. 1974. Oxidation of ilmenite and the product morphology. *High temperature science*, 6, pp. 323-341.
- Ryall, P.J.C. and Hall, J.M. 1980. Iron loss in titanomagnetites during low temperature oxidation, *J. Geomag. Geoelectr.*, 32, pp. 661-669.
- Readman, P.W. and O'Reilly, W. 1972. Magnetic properties of oxidised (cation-deficient) titanomagnetites (Fe, Ti, $)_3O_4$, *J. Geomag. Geoelectr.*, 24, pp. 69-90.
- Sinha, H.N. 1984. Hydrochloric acid leaching of ilmenite, Proc. Symp. on *Extractive Metallurgy*, AusIMM, Melbourne (Australia), pp. 163-168.
- Tikkanen, M.H.A. and Tholand, N.K.G. 1960. Extraction of iron from iron-bearing titaniferous raw materials. *US Pat. 2,961,298*, 22 Nov.
- Tikkanen, M.H., Tyynalä, T. and Vuoristo, E. 1964. Reducing pressure leaching of an ilmenite concentrate. In: *Unit processes in hydrometallurgy*. Ed. M.E. Wadsworth and Davis, Gordon and Breach Science Publ., New York (USA), pp. 269-283.
- Van Dyk, J.P. 1996. Evaluation of processes that upgrade titanium bearing slags by utilising phosphate additions. *MEng dissertation*, University of Pretoria (South Africa).
- Walpole, E.A. (1993). Acid Regeneration, *World patent WO 9316000*, Aug 19.
- Webster, A.H. and Bright, N.F.H. 1961. The system iron-titanium oxygen at 1200°C and oxygen partial pressures between 1 atm and $2x10^{-14}$ atm. *J. Am. Ceram. Soc.*, 44, pp. 110-116.